**ISTANBUL TECHNICAL UNIVERSITY ★ GRADUATE SCHOOL OF SCIENCE ENGINEERING AND TECHNOLOGY**

# ANALYSIS OF 5 KW ORC SYSTEM OPERATING WITH R245FA AND PLATE TYPE EVAPORATOR AND CONDENSER

**M.Sc. THESIS**

**Yashar AMROLLAHI FARZI**

**Department of Mechanical Engineering**

**Heat and Fluid Program**

**MAY 2018**

**ISTANBUL TECHNICAL UNIVERSITY ★ GRADUATE SCHOOL OF SCIENCE ENGINEERING AND TECHNOLOGY**

# ANALYSIS OF 5 KW ORC SYSTEM OPERATING WITH R245FA AND PLATE TYPE EVAPORATOR AND CONDENSER

**M.Sc. THESIS**

**Yashar AMROLLAHI FARZI**
**(503141136)**

**Department of Mechanical Engineering**

**Heat and Fluid Program**

**Thesis Advisor: Prof. Dr. Mustafa Özdemir**

**MAY 2018**

**İSTANBUL TEKNİK ÜNİVERSİTESİ ★ FEN BİLİMLERİ ENSTİTÜSÜ**

# R245FA VE PLAKALI EVAPORATÖR VE KONDANSERLE ÇALIŞAN 5 KW GÜCÜNDEKİ ORC SİSTEMİNİN ANALİZİ

**YÜKSEK LİSANS TEZİ**

**Yashar AMROLLAHI FARZI**
**(503141136)**

**Makina Mühendisliği**

**Isı Akışkan Programı**

**Tez Danışmanı: Prof. Dr. Mustafa ÖZDEMİR**

**MAYIS 2018**

Yashar AMROLLAHI FARZI, a M.Sc. student of ITU Graduate School of Science Engineering and Technology student ID 503141136, successfully defended the thesis entitled "ANALYSIS OF 5 KW ORC SYSTEM OPERATING WITH R245FA AND PLATE TYPE EVAPORATOR AND CONDENSER", which he prepared after fulfilling the requirements specified in the associated legislations, before the jury whose signatures are down below.

| | | |
|---|---|---|
| **Thesis Advisor :** | **Prof. Dr. Mustafa Özdemir**<br>İstanbul Technical University | ..... |
| **Jury Members :** | **Prof. Dr. İsmail Cem Parmaksızoğlu**<br>İstanbul Technical University | ..... |
| | **Prof. Dr. Özgür Atayılmaz**<br>Yıldız Technical University | ..... |

**Date of Submission : 24 April 2018**
**Date of Defense : 15 May 2018**

***To my dear family,***

## FOREWORD

I would like to express my deep appreciation and thanks for my advisor, Prof. Dr. Mustafa ÖZDEMİR. This was impossible without his warm guidance, support and encouragement during the entire thesis study.

At the end, I would like to thanks my family for their warm support and love in my life.

April 2018

Yashar AMROLLAHI FARZI

(Mechanical engineer)

**TABLE OF CONTENTS**

**Page**

## ABBREVIATIONS

**ORC** : Organic Rankine Cycle
**GWP** **:** Global Warming Potential
**ODP** **:** Ozone Depletion Potential
**HEX** **:** Heat Exchanger
**HTC** **:** Heat Transfer Coefficient
**PHE** **:** Plate Heat Exchanger
**ITD** **:** Inlet Temperature Difference

**SYMBOLS**

| | |
|---|---|
| **v** | **:** Velocity |
| $\boldsymbol{P}$ | **:** Pressure |
| $\boldsymbol{\rho}$ | **:** Density |
| $\boldsymbol{\rho_l}$ | **:** Density (saturated liquid) |
| $\boldsymbol{\rho_v}$ | **:** Density (saturated vapor) |
| $\boldsymbol{\mu}$ | **:** Dynamic viscosity |
| $\boldsymbol{\mu_v}$ | **:** Dynamic viscosity (saturated vapor) |
| $\boldsymbol{\mu_l}$ | **:** Dynamic viscosity (saturated liquid) |
| $\boldsymbol{2a}$ | **:** Spacing between plates |
| $\boldsymbol{\eta}$ | **:** Efficiency |
| **L** | **:** Plate length |
| $\boldsymbol{f}$ | **:** Friction factor |
| **T** | **:** Temperature |
| $\boldsymbol{\nu}$ | **:** Kinematic viscosity |
| $\boldsymbol{w}$ | **:** Plate Width |
| $\boldsymbol{Re}$ | **:** Reynolds number |
| $\boldsymbol{We}$ | **:** Weber number |
| $\boldsymbol{Bo}$ | **:** Boil number |
| $\boldsymbol{Bd}$ | **:** Bond number |
| $\boldsymbol{T_w}$ | **:** Wall Temperature |
| $\boldsymbol{\beta}$ | **:** Chevron Angle |
| $\boldsymbol{\phi}$ | **:** Enlargement factor |
| $\boldsymbol{N_t}$ | **:** Number of plates |
| $\boldsymbol{D_h}$ | **:** Hydraulic diameter |
| $\boldsymbol{x}$ | **:** Quality |
| $\boldsymbol{h}$ | **:** Enthalpy |
| $\boldsymbol{\nu}$ | **:** Specific Volume |
| $\boldsymbol{G}$ | **:** Mass Flux |
| $\boldsymbol{s}$ | **:** Entropy |
| **Ɛ** | **:** Heat exchanger efficiency |
| **NTU** | **:** Number of Transfer Units |
| **U** | **:** Overall heat transfer coefficient |
| $\boldsymbol{R_c}$ | **:** Fouling constant on cold side |
| $\boldsymbol{R_h}$ | **:** Fouling constant on hot side |
| $\boldsymbol{A_c}$ | **:** Cross section area |
| $\boldsymbol{V}$ | **:** Velocity |
| $\boldsymbol{Q_c}$ | **:** Condenser capacity |
| $\boldsymbol{Q_h}$ | **:** Evaporator capacity |
| $\boldsymbol{W_{exp}}$ | **:** Expander work |
| $\boldsymbol{T_{ex}}$ | **:** Expansion valve outlet temperature |

**LIST OF TABLES**

**LIST OF FIGURES**

**Page**

**ANALYSIS OF 5 KW ORC SYSTEM OPERATING WITH R245FA AND PLATE TYPE EVAPORATOR AND CONDENSER**

## SUMMARY

In today's world, the major part of the electrical energy is produced by consumption of hydrocarbon fuels in combined power plants. The thermal efficiency of these plants is higher, because of high source temperature that is occurred by burning of hydrocarbon fuels. Utilization of natural sources like solar and geothermal energies and industrial waste heat (flue gases, exhaust gases, etc.) had not been economically efficient because of their low temperature. However, through previous years by using hydrocarbon-based fluids instead of water, efforts are in progress on the utilization of a steam power system called ORC, which utilizes low-grade heat sources. Especially ORC systems are established for utilization of geothermal sources.

In this study, a 5 kW ORC heat engine is modeled. Evaporator and condenser of the engine are chosen as plate type heat exchanger (HEX). The working fluid is selected as R245fa. This ORC system consists of evaporator, condenser, expander and the pump; in addition to these components, the expansion valve is added which is basically used in times of start-up and for adjusting the power output of the system.

In this work, the heat source is specified as pressurized water of 125 C temperature based on Turkey's geothermal resources. Heat sink, however, is specified 25 C based on the climate of the country.

Flow and heat transfer formulations are made for all of the units and coded in Mathcad program to parametrically perform thermal calculations.

Working fluid is considered as compressed liquid at inlet, and superheated vapor at outlet in the formulation of the evaporator. Since the evaporator is considered as a single pass plate heat exchanger (PHE), starting points of boiling and superheating in the plate channels are calculated in analyzing of the evaporator. Suitable friction factor

and Nusselt correlations are chosen for single and two-phase regions in the evaporator and condenser.

Evaporation temperature of 75.2 C and condensation temperature of 40 C values are selected as design conditions for our system. Pump and expander efficiencies are set as 35.6% and 75% , respectively.

Evaporator and condenser capacities are calculated as 80.10 kW, and 75.10 kW, respectively. The thermal efficiency of the ORC cycle is obtained as 6.242% while pump and expander powers are 0.3 kW and 5.3 kW. On the other hand, the final condenser power is calculated as 80.40 kW when the working fluid passes completely through the expansion valve.

For two different chevron angles of 45 and 60 degrees, heat transfer coefficients (HTC) and pressure losses are compared with each other. Plates with 60-degree chevron angles have higher HTC and higher pressure loss then 45-degree chevron angle. Pressure loss in HEXs decreases cyle thermal efficiency by 0.444% for chevron angle of 45 degrees and 0.561% for chevron angle of 60 degrees.

Evaporator and condenser calculations performed by taking into account the plate number and dimensions. Required hot water mass flow rate with 125 C temperature is 0.901 kg/s in evaporator. For condenser, however, required cold water mass flow rate with 25 C temperature is accuired as 2.55 kg/s and required cold water mass flow rate when fluid passes expansion valve is obtained as 2.62 kg/s.

In design conditions, HEX efficiencies are obtained as 0.53 for preheat region, 0.3 for evaporator region, and 0.98 for superheat region. In case of the condenser, for desuperheater region efficiency is obtained as 0.85 and for condenser obtained as 0.6.

Regarding the effect of cold water temperature change on condenser, results indicate that cold water temperature varies between 21-28 C. Fully condensed fluid at condenser outlet can be maintained by adjusting the mass flow rate of cold water in this range of temperature. However, extra condenser is required for water temperatures over 28 C, because of excessive required water mass flow rate to have fully condensed fluid at the condenser outlet.

Increase in pump and expander isentropic efficiencies can positively affect cycle thermal efficiency. Increasing of evaporation temperature and decreasing of condensation temperature can also improve thermal efficiency.

Overall area of HEXs for the same output power is decreasing by increasing of evaporation temperature until 95 C.

## R245FA VE PLAKALI EVAPORATÖR VE KONDANSERLE ÇALIŞAN 5 KW GÜCÜNDEKİ ORC SİSTEMİNİN ANALİZİ

## ÖZET

Dünyamızda elektrik enerjisinin üretiminin çok önemli bir kısmı hidrokarbon yakıtlar kullanılarak bileşik güç santrallerinde elde edilmektedir. Bu santrallerde yakıtın yakılmasıyla çok yüksek kaynak sıcaklıklarına erişildiğinden ısıl verim de yüksek olmaktadır. Güneş enerjisi, jeotermal enerji gibi doğal kaynakların ve endüstriyel atık ısıların (baca gazları, egzos gazları, vb) sıcaklıklarının düşük olması sebebiyle elektrik enerjisi üretiminde kullanılması uzun yıllar ekonomik olmamıştır. Ancak, son yıllarda iş yapan akışkan olarak su yerine hidrokarbon esaslı akışkanların kullanıldığı ve düşük sıcaklıktaki ısı kaynaklarını kullanan ORC isimli buhar santralleri üzerinde çalışmalar yapılmaktadır. Özellikle düşük sıcaklıktaki jeotermal enerjinin kullanıldığı ORC tesisleri kurulmuştur.

Bu çalışmada, ele alınan 5 kW'lık ORC ısı makinası modellemesi yapılmaktadır. Makinanın evaporatör ve kondenserleri plakalı ısı değiştirici tipinde ve iş yapan akışkan olarak da R245fa seçilmiştir. Evaporatör, kondenser, genişletici ünite ve pompadan oluşan ORC sistemine bu çalışmada bir de kısılma vanası eklenmiştir. Kısılma vanası esas olarak sistemin ilk çalışma durumunda veya güç ayarlamasında kullanılmaktadır.

Çalışmada Türkiye'nin jeotermal enerji kaynakları gözönüne alınarak sıcak ısı kaynağı 125 C sıcaklıkta basınçlı su ve soğuk ısı kaynağı olarak ise 25 C sıcaklıkta su seçilmiştir.

ORC sisteminin bütün elemanlarına ait akış ve ısı geçişi formülasyonu yapılmış ve Mathcad üzerinde program yazılarak termodinamik ve ısıl hesaplar parametrik olarak hesaplanmıştır.

Evaporatör ünitesinin formülasyonunda, akışkanın sıkıştırılmış sıvı halinde girdiği ve kızgın buhar olarak çıktığı gözönüne alınmıştır. Plakalı evaporatörde sıcak ve soğuk akışkanlar tek geçişli olarak ele alındığından, akışkanın plakanın hangi noktasında kaynamaya ve kızmaya başladığı hesaplanmaktadır. Evaporatör ve kondanserin tek fazlı ve çok fazlı olduğu bölgeleri için farklı uygun sürtünme ve Nusselt korelasyonları gözönüne alınmaktadır.

Dizayn şartları olarak evaporasyon sıcaklığı 75 C, kondenser sıcaklığı 40 C, pompa ve genişletici verimleri %35.6 ve %75 seçilmiştir.

Elde edilen evaporatör gücü 80.10 kW, tasarım şartlarında genişleticiyi kullanırken kondenser gücü 75,10 kW, pompa gücü 0,3 kW, genişletici gücü 5,3 kW değerlerinde elde edilmiştir. Çevrimin ısıl verimi % 6,242 olarak hesaplanmıştır. Kısılma vanası kullanılırken gerekli kondenser gücü 80,40 kW olarak elde edilmiştir.

Iki farklı çevron açısı için ısı taşınım katsayıları birbiriyle karşılaştırılmış. 60 derecelik plakalı ısı değiştiricinin daha yüksek ısı taşınım katsayısı olduğu ama aynı halde daha yüksek basınç kaybı olduğu da gösterilmektedir. Isı değiştiricilerindeki basınç kayıplarının çevrimin ısıl verimini azalttığı, 45 derece çevron açısı için verimin %0,444 ve 60 derece çevron açısı için de %0,561 olduğu tespit edilmiştir.

Evaporatör ve kondenser hesabında levha sayısı, levha eni ve boyu dikkate alınarak detay hesaplamalar yapılmaktadır. Evaporatör için gerekli 125 C deki sıcak su debisi 0.901 kg/s olarak tespit edilmiştir.

Kondenser hesabında geometrik yapı belirlendikten sonra 25 C soğuk su sıcaklığına göre hesaplamalar yapılmış ve soğuk su debisinin 2,55 kg/s olması gerektiği bulunmuştur. Akışkanın kısılma vanasından geçtiği durumlarda soğuk su debisinin 2,62 kg/s olduğu tespit edilmiştir.

Dizayn şartlarında evaporatör ve kondenser etkenlikleri preheater kısmı için 0,53, evaperatör kısmı için 0,30 ve superheater kısmı için 0,98 , desuperheater kısmı için 0,85 ve kondanser için de 0,60 olduğu tespit edilmiştir.

Soğuk su debisi ve sıcaklığının sisteme etkisi incelenmiş ve kondanserin soğuk suyun 21-28 C aralıklarında çalışabildiği gösterilmiştir. Soğuk su sıcaklığının 28 C dereceyi geçtiği durumda, kondanser çıkışında tamamen kondans olmuş akışkan elde etmek için ekstra kondansere gerek olduğu belirlenmiştir.

Pompa ve genişleticinin isentropik verim artışları çevrimin ısıl verimini pozitif yönde etkilemektedir. Bu durum çizilen eğrilerle ortaya konulmuştur.

Evaporasyon sıcaklığın artışı ve kondanser sıcaklığının düşüşü çevrimin ısıl verimini arttırdığı eğrilerle gösterilmiştir.

Evaporasyon sıcaklığı 95 C ye kadar arttığında üretilen aynı güç için evaporatör ve kondanserin gerekli toplam alanı azalmaktadır. Bu alan 95 C de bir minimumdan geçmektedir. Böylece, kondanser sıcaklığı, sıcak ve soğuk ısı kaynak sıcaklıkları, pompa ve genişletici verimleri aynı iken toplam ısı geciş alanının minimum olduğu bir

durumun olduğu gösterilmiştir.  Evaporator ve kondenser etkenlikleri de evaporasyon sıcaklığının artışıyla artmaktadır.

## 1. INTRODUCTION

Nowadays, energy crisis and climate change concerns are the two of the challenges that present and future generations may probably face. World's oil reservoirs are depleting fast by today's rate of consumption, high amount of fossil fuel consumption can negatively affect the climate change. Without decisive planning and actions, these situations are going to be harsher and affect lives of millions of people.

From last few years, these increasing environmental and energy crisis concerns have sped up research work in the field of better implementation of the energy resources. Exhaust gases of power production plants are affecting global warming and greenhouse effect [1]. Utilization of the low-grade sources and waste heat recovery can notably decrease the greenhouse gas emissions. Low-grade is available in different shapes, including waste heat of industrial plants, heavy-duty vehicles and the renewable sources like geothermal and solar energy. The temperatures of these resources are generally below than 400-550°C [2].

Conventional Rankine cycle with water as working fluid is not suitable for utilization of these sources, because of water's thermo-physical properties [3]. So using the organic fluids like refrigerants or hydrocarbons that have better-suited properties to these temperatures is necessary. Rankine cycle by organic fluid as working fluid is called ORC (Organic Rankine Cycle). Application of Organic Rankine Cycle (ORC) for utilization of low-grade heat sources shown to be one of the effective ways of using low-grade sources. ORC systems operation are of similar to conventional Rankine cycles, however efficiencies are quite lower comparing conventional Rankine cycles, which are generally between 32-42%, and Brayton cycles with 32-38% [4]

In past years, many ORC units successfully employed in different regions throughout the world but requirement for better efficiency and cost reduction challenges remain. Economic viability relies on both cycle efficiency and capital cost of the ORC unit, which is highly related to heat exchangers size. Evaporator and condenser size mostly correlated with the type of working fluid and its heat transfer and pressure drop behavior in the heat exchanger.

Currently, low efficiency and the high cost of ORC systems affect the wide spread extension of these systems.

In the first chapter, in order to introduce the history of ORC, short historical records related to ORC are briefed in subchapter 1.1. Early commercial plants and active companies in the ORC sector are explained in 1.2. Literature survey of the thesis explained in subchapter 1.3. A sample study of ORC cost explained in 1.4. Motivating factors and aim of the thesis are put into words in 1.5. Finally, contents of the chapters are shortly explained in the subchapter 1.6 to point out an overview of the thesis.

### 1.1 Birth and History of ORC

The history of the Organic Rankine Cycle (ORC) progress returns to the early 19th century and continues until the ORC power systems became an important recess market in the power industry of 21st century. The ORC systems have a relatively long history, back in the first half of the 19th century, nearly a century after the creation of the steam engine. The idea of using the organic fluid as operating fluid in power cycles return to Sadi Carnot disquisition in the year 1824 by the name of "Reflections on the motive of fire"[5]; in which he suggests using of other substances as substitutes for water.

However, at that time because of different reasons such as expansiveness of operation and technological drawbacks, Carnot's message was not heard very much, so we must deduce that Carnot's message was actually for engineers of a generation yet to come with the more technologically advanced assets; ORC systems appearance has to wait until the 1930s.

The early 19th century was the interval of the great progress of the reciprocating steam engines. Existing reciprocating steam engines were the basis of progress of ORC systems. The use of substitute fluids can be detected back to the pressure restriction of the boilers at that time [5].

The challenge to reach acceptable condenser vacuum, resulted in relatively high heat sink temperatures because of insufficient sealing techniques. Utilization of the heat rejected in the condensation process is the point in which of organic working fluids owes its emergence [5].

### 1.2 Early Commercial Plants

Some examples of commercialized plants [5] through past years are mentioned in this section.

1-In 1952 at Kiabukawa in Congo, a small 200 kW ORC unit used water at 91 C from a spring and supplied electric power to a mine for a number of years.

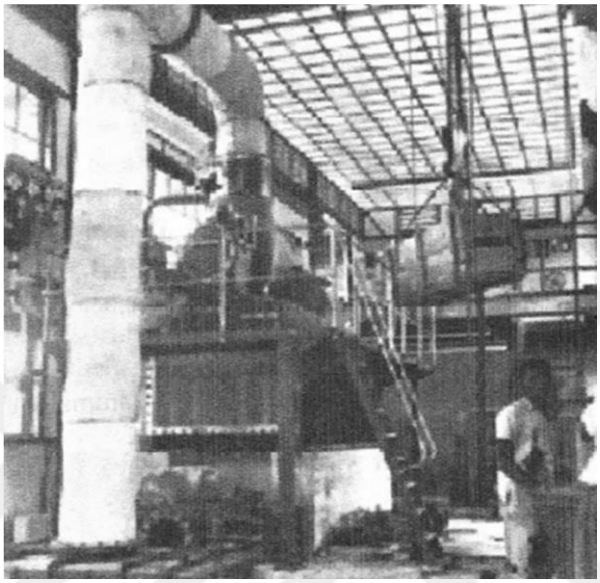

**Figure 1.1:** Kiabukawa 200 kW unit, 1952 **[5]**.

2. 1966, Ormat 0.6 kW solar turbogenerator using dichlorobenzene driving an electrical submerged irrigation pump in Mali, Africa.

3. 1967 a 500 kW geothermal plant, using R12, was started in Paratuka, Kamtchatka in the USSR, now Russia

4. 1979, at the Kashima steel Works, Kawasaki, Japan, completed a 2900 kW ORC system for process heat recovery using Freon 11 In another steel mill at Kimitsu, Mitsui and Thermo Electron built an 11.5 MW ORC using Fluorinol 85 .

5. 1979, Ormat build a 150 kW solar pond power unit


**Figure 1.2:** The 150 kW solar pond and power unit at the Dead Sea, Israel **[5]**.

6. 1979, McCabe built a commercial 12.5 MW cascading ORC with two fluids, isopentane and isobutane, in East Mesa, California. The cooling water for the condensers was cooled in evaporation ponds. The plant was designed by J. Hilbert Anderson and used York expanders.

7. 1982, Ormat installed 15 kW geothermal power unit on a well drilled by CFE (Mexican utility) using Freon 113.

8. 1982, Ormat completed a 5 MW solar pond power plant which operated for seven years.

### 1.2.1 Active ORC manufacturers

Several ORC manufacturers are active and well known in this sector. We are going to mention them by names and briefly explain introduction few of them as follows [5].

Ormat, Turboden, Adoratec, Atlas Copco, Electratherm, Exergy, General Electric, GMK, Triogen Company (Triogen), Turbine air systems (TAS), United Technologies (Pratt and Whitney) are some of the main active companies in this sector. First two company (Ormat, Turboden) have a relatively long past, But the rest of the companies recently entered into this sector.

*Omrat*

Ormat was founded by Lucien and Dita Bronicki in 1964 with an agreement with National Preparedness Leadership Initiative (NPLI) to implement Lucien's work and the right to use the patented new cycle. The company is a pure player in renewable energy, a leading vertically integrated company engaged in the geothermal and recovered energy power business. It designs, develops, owns, and operates geothermal and recovered energy-based power plants predominantly using ORC units designed and manufactured by it.

*Turboden*

Mario Gaia founded Turboden in 1980, with the specific company object of researching, designing, manufacturing, commissioning, and servicing organic Rankine cycle turbogenerators.

*ElectraTherm*

ElectraTherm incorporated in 2005 and is headquartered in Reno, Nevada. Power Generator generates clean electricity from low-grade waste heat utilizing ORC and proprietary technologies. The machines are fully packaged (Fig.3), with outputs up to 110 kW for distributed power generation from low-grade waste heat utilizing water cooled ORC and proprietary technologies.


**Figure 1.3** ElectraTherm Power generator **[5]**.

### 1.3 Literature Survey

Currently, large-scale amount of low-temperature energies from different sources like renewable and waste heat of industrial processes are available and not effectively used. By benefitting from these resources, fossil fuel usage and greenhouse gases [1] can considerably be reduced. Nearly 60% resultant waste heat from industrial processes is lower than 230°C [2, 6]. The Organic Rankine Cycle (ORC) appraised as a practical technology for effective recovery of low-grade heat sources and has a long history from the 20$^{th}$ century [5]. The ORC system operation is quite alike to conventional steam Rankine cycle with lower efficiency [4, 18], but as replacement of water, which is not suitable to use in low temperatures [3], refrigerants and hydrocarbons are used as working fluids. ORC systems can be categorized into three groups by their operating pressure to subcritical, trans-critical and supercritical [19, 20]. Small and large-scale ORC units have been successfully used in industry and remote areas for the production of power [7] however, the requirement for higher efficiency and cost reduction still not completely resolved [8]. The economic feasibility [14, 15] and unit cost [16, 17] of an ORC plant is highly correlated with the heat exchanger size [9].

Organic fluid properties [23, 24] have an immense impact on performance, working conditions of the ORC system, environmental effect and economic practicality [10]. Heat source temperature depend on geothermal resources of Turkey (for our case) [21] on the other hand, heat sink temperature depends on the climate of the country [22].

Plate heat exchangers (PHE) have relatively lower volume comparing other types of HEXs because of higher area per unit volume, which makes them particularly suited for installation in limited spaces, especially for small ORC systems. In PHEs, usually there is a counter-flow regime [26] that improves heat transfer performance. The evaporator and condenser size depends on the heat transfer and pressure drop characteristics of the working fluids of the ORC, predicted using the experimental correlations. These correlations are sensitive to the geometry of heat exchanger [31], operating conditions and working fluid [25]. Correlations for flow boiling of R245fa, a commercial working fluid used in organic Rankine cycle, in plate heat exchanger with chevron angle of 45-degree and 60-degree is obtained by experimental study [11]. Correlations of heat transfer and pressure drop are proposed for both chevron angles. Due to the increase in turbulence and secondary flow in 60 degree chevron angle, a higher value of HTC and higher frictional pressure drop have been observed [11].

Positive displacement expanders are widely used in ORC units especially in low capacities [27]. Different types of expanders have their own advantages and disadvantages [28]. Pumps mechanical efficiency for ORC systems can vary from 31% to 81% [33]. Regarding scroll expanders, a recently designed scroll expander has mechanical efficiency of near 75% [30] but the range of the efficiency for scroll expanders is between 61-75% [34].

Heat transfer with considering fouling [32] in HEX and pressure drop in plate type condenser for R245fa and mixtures of this fluid are investigated [12]. Higher evaporator pressure can result in less overall heat exchanger area in ORC. This includes the total heat transfer area in evaporator, condenser and desuperheater [13].

### 1.4 ORC System Cost

Based on an analysis [15] on a **micro CHP unit** with 5kW power output and efficiency of 8% displayed in economic performance curve in Figure 4. The Graph below depicts electricity production price vs operational hours. In this Figure, vertical line depicts operational hours, horizontal line shows heat price. (Heat price/revenue depicts the cost of heat, since this unit consumes about 90% of heat and 10% of its waste heat for heating purposes; this number affects its total revenue). Cost of produced power is displayed in Ct (1Ct means 0.01 €/KWh). With the operating time of 7500 hours, electricity production price will yield about 0.105 €/KWh while typical heat price is assumed to be 0.09€/KWh [14].

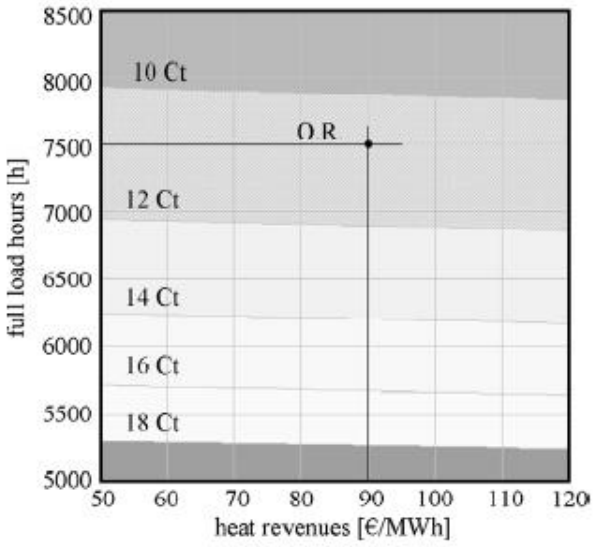


**Figure 1.4:** Electricity price for a 5kW micro ORC system (1Ct means 0.01 €/KWh, OR: Operation Range) **[15]**.

Micro ORC CHP unit applications in distant areas which uses solar energy as heat source will decrease the electricity price down to about 0.14 $/KWh that is quiet lower than diesel based electricity price of 0.3$/KWh [15]. These applications can be a solution to heat and electricity needs and will notably help in lowering the C02 emission.

### 1.4.1 Sample cost analysis of 10 kW ORC system

A sample system with its characteristics depicted in Fig 5. Total price of below ORC package with a generator approximated as 30,000 $. Electricity price in Turkey is about 0.1 USD cents/kWh [16]. With 8 hour daily operation time and 350 days a year. Revenue return for covering initial cost can take up to 12.5 years. Therefore, we can conclude that cost reduction for ORC units is essential, so the final price become attractive to investors in such systems.

| Description | Rack Mounted<br>DC or AC Output |
|---|---|
| Net Power Output (Based on R245fa Genetron) | 10,000 Watts (10 kw) |
| Generator (add on) Direct Shaft Drive 1,800 - 3,600 RPM | Optional DC or AC 50/60hz |
| Evaporator Flow - gpm (liters/min) | 22 gpm @ 194 F less 25 F outlet<br>(83 lpm @ 90C less 15 C outlet) |
| Condenser Flow - gpm (liters/min) | 44 gpm @ 59 F plus 25 F outlet<br>(166 lpm @ 15C plus 15 C outlet) |
| BTU Input (based on 35,000 btu/kw heat rate) | 420,000 btu/hr |
| Frame Version Only - Dimensions (uncrated) and Weight<br>2 x 2 x 4 ft (400 lbs) approx. | 610 mm x 610 mm x 1220 mm<br>(181 kg) |
| Operating Sound (Depends on Working Fluid) | 65dBA @ 10 m (33 ft) |
| Inlet and Outlet Pipe Sizes | 2 inch (51 mm) |
| Application Considerations | Direct Shaft Drive |
| Waste Heat Applications | Biomass, Engine Waste Heat, Solar,<br>Geothermal, Industrial, Boiler |
| Time to Manufacture (approximate) | 12 weeks+ |
| Complete ORC Package (does not include generator) | $25,000 |
| Turbine Only (for steam, refrigerant, etc.) | Approx $15,000 - Market Price |
| 12 kw 400 V DC to AC Inverter (50/60hz available in 1 or 3 Phase) | Approx $6,000 - Market Price |
| The Infinity Turbine IT10 is experimental and designed for 80-120C input waste heat (liquid form). | |

**Figure 1.5:** Infinity Turbine IT10 ORC system **[17]**.

## 1.5 Motivation and Thesis Aim

Several reasons motivated me for this subject; we live in a world in which, global warming and energy shortage crises continue to affect lives of millions of people in ways that could lead to possible unrest around the globe. ORC presents a way to use low temperature sources such as exhaust gases of conventional power plants and the renewable resources for example geothermal and solar energies, to provide power for clean water extraction or purification of sea waters or to provide electricity for these areas without making global warming any harsher.

This thesis's aim and objective is to analyze a small ORC system. For this thesis, a computer code developed in Mathcad program, and related formulas and correlations codded in it to investigate expander and pump's mechanical efficiency, evaporation and condensation temperature effects on cycle thermal efficiency. The effect of cold source temperature change on the inlet cold water mass flow rate to condenser in order to have fully condensed fluid at the condenser outlet, chevron angle effect on heat transfer and frictional pressure drop, and to analyze the effect of evaporation temperature on the overall area of HEXs.

## 1.6 Brief Information About Chapters

This thesis comprises four chapters. First chapter is related to the introduction for ORC, in which some of ORC history and some information about known ORC plants and companies in this sector are provided. Second chapter is about theoretical basis of the ORC; in this chapter informations about thermodynamics of Rankine cycle, design condition, necessary equipment and basic science of heat transfer are presented. Chapter 3 is about explanation of the determination of the design parameters, calculation procedure of heat transfer and pressure loss in Mathcad program for each equipment. And in chapter four results and some discussion of the analysis are mentioned. Finally, in chapter five conclusion about the study is presented.

# 2. THEORETICAL BASIS OF ORGANIC RANKINE CYCLE

In order to introduce an ORC system, thermodynamic processes of the cycle, information about different organic fluids, different components of the system and related formulas of fluid flow and heat transfer are needed to be described.

In this chapter, in 2.1 main processes of an ideal basic Rankine cycle are described. Then types of ORC by the sort of operating pressure are discussed in 2.2. In the subchapter 2.3, basic concepts in designing of ORC such as heat source and heat sink are defined. Subchapter 2.4 is about organic fluids, main criterions in selecting a fluid are discussed and also their physical and safety data are mentioned. In 2.5 common heat exchangers and our chosen exchanger are discussed then heat transfer and pressure drop formulations are described. In the 2.6 different types of expanders and our chosen expander are explained. Finally in 2.7 informations about pump and related formulations are mentioned.

## 2.1 Ideal Basic Rankine Cycle

Rankine cycle is known as one of the viable power cycles. Water is the difference between ORC and conventional Rankine cycle, which is suitable for high temperature heat sources because of its thermo physical properties so fluids such as hydrocarbons and refrigerants are used in ORCs. Main four processes in an ideal Rankine cycle are as follow.

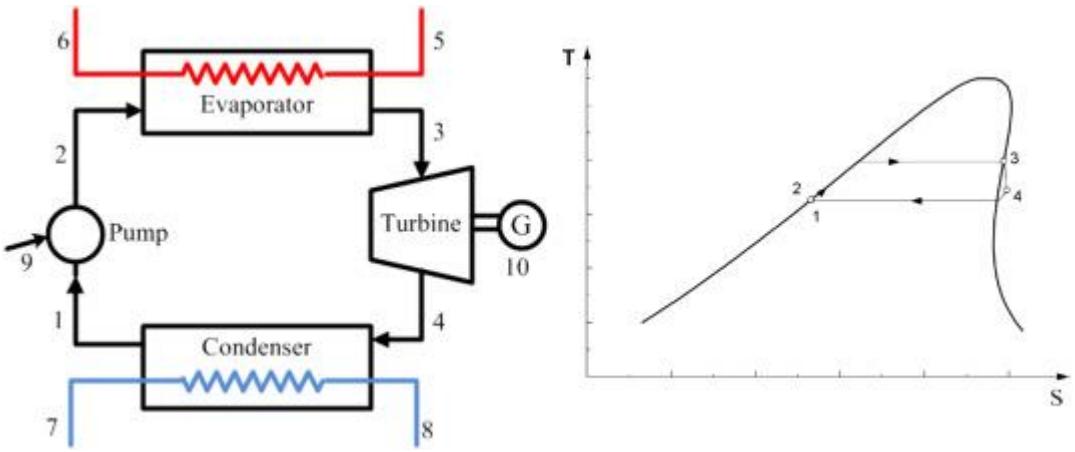


**Figure 2.1:** ORC schematic and T-s diagram **[18]**.

2-3 **Isobaric Heat Addition**.: High-pressure liquid (water in Rankine cycles) go through an isobaric heat transfer process in which at first it enters the evaporator from the feed pump (1). And then absorbs heat to reach the saturation temperature, after that with extra heating evaporation of the liquid takes place and this evaporation continues until liquid fluid is fully converted to saturated steam and after that if needed to superheated state(3).

3-4 **Isentropic Expansion**. In this process, the expansion of steam in expander (Turbine in this case) takes place then it may convert to electricity using a generator. In organic fluids, depending on the T-S curve of the fluid, state after expansion is mainly fall in superheat region.

4-1 **Isobaric Heat Rejection**. This process is actually reverse process of isobaric heat addition. Vapor exits the expander in superheated state (4) first desuperheats and then condenses at lower pressure. In conventional Rankine cycles, which operate with water, the exiting steam-liquid pressure is lower than atmospheric pressure in a well-designed and maintained condenser.

1-2 **Isentropic Compression**. The condensate liquid pressure increases in the feed pump. In ORC cycle, pump work depend on the characteristics of the fluid. However in conventional Rankine cycle since the water specific volume is low, the work required by pump is relatively small therefore in thermodynamic calculation it is usually neglected.

## 2.2 Types of Organic Rankine Cycle

Organic Rankine Cycles can be categorized into three types based on the pressure of operation of four processes.

Subcritical ORC: In this cycle, all of the processes take place at a pressure lower than the critical pressure for the operating fluid.

Trans-critical ORC: In this cycle, process of heat addition occurs at a pressure higher than critical pressure and heat rejection process happens at a pressure lower than critical pressure. Compression and expansion occur at a pressure between two pressure levels.

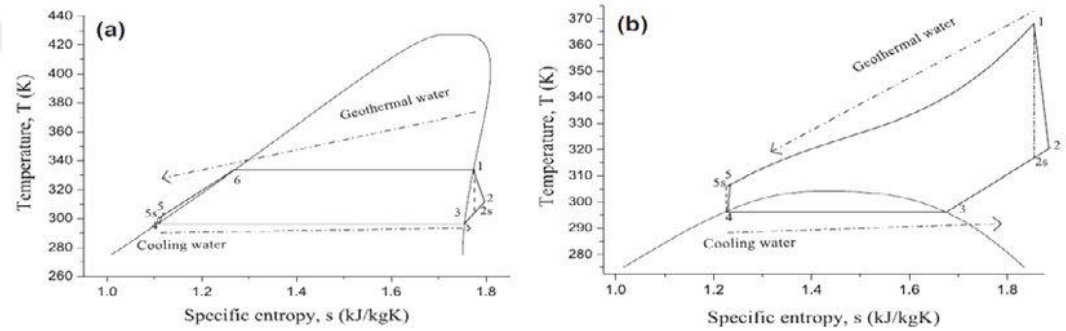


**Figure 2.1 :** a) Subcritical ORC, b) Trans-critical ORC **[19]**.

Supercritical ORC: In this cycle, all of the processes occur at a pressure higher than the critical pressure for the operating fluid.

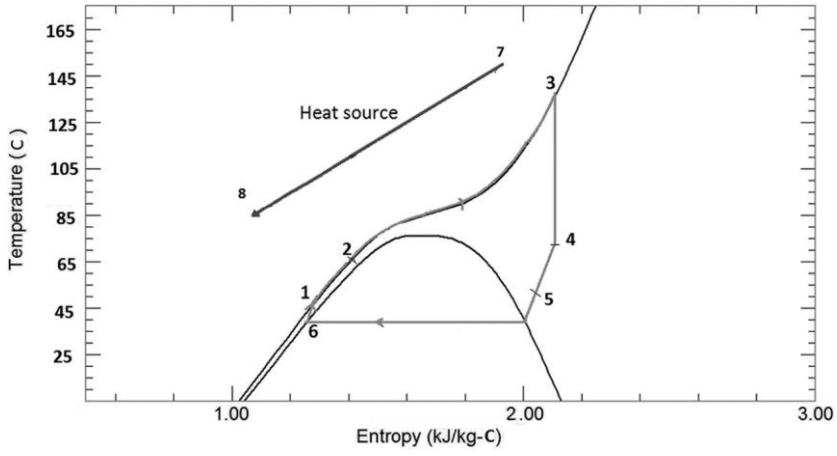


**Figure 2.2:** Supercritical ORC **[20]**.

## 2.3 Basic Concepts in Designing Organic Rankine Power Cycles

In designing an ORC cycle, heat source and heat sink temperature are selected on the basis of different parameters. Different types of heat sources are available to use in ORC systems (Fig.9) and based on the available sources and assets, any of them can be used in ORC units. In addition, heat sink temperature is selected by considering environmental condition. Evaporation temperature choice is also vital to ORC performance.

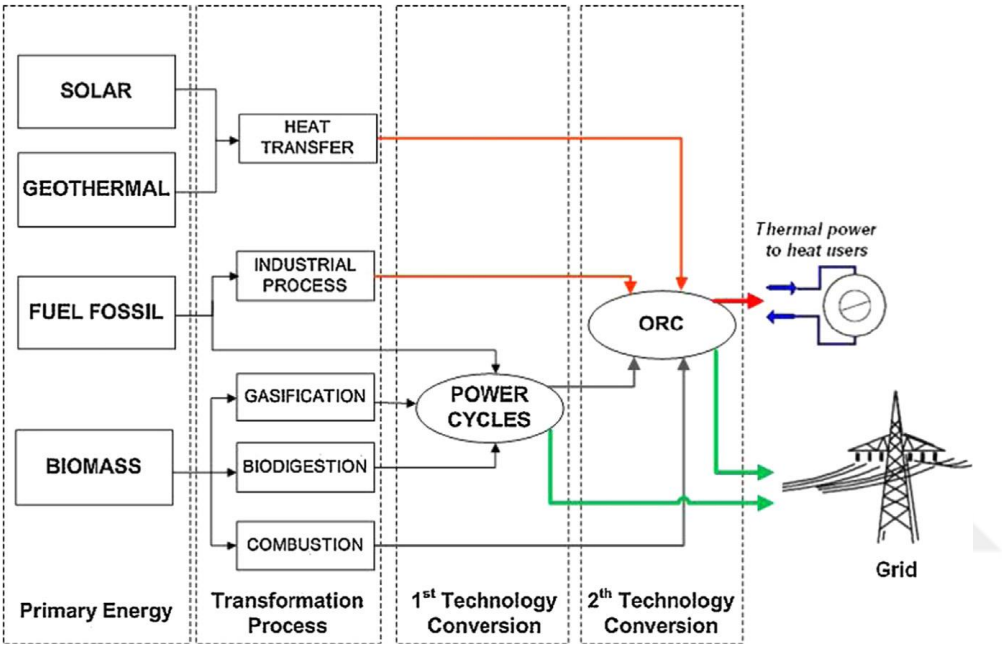


**Figure 2.3:** ORC systems using different heat sources **[21]**.

### 2.3.1 Defining heat source and heat sink

Different heat source temperatures are usable for ORC based on type of the source. Heat temperature from industrial applications, power waste heat, geothermal, solar collector, solar pond and biomass are the types explained in table 1. Hydrothermal reservoirs contain heated water or steam, which can directly exchange heat with ORC systems, mainly have temperature range of 80-180 °C [2].

In Table 2.1, heat sources are categorized into three types. A, B-open, B-closed (explained in Fig.9). Definitions of these terms are: A means cooling cycle, hot fluid enters the HEX, In B type, a medium fluid absorbs heat from the source fluid and enters the HEX

**Table 2.1:** Source temperatures by heat source type **[2]**.

| Heat Source | Type | Source Temperature |
|---|---|---|
| Industry | **A,B-Open-Closed** | **80-500 °C, Mostly 200-300°C** |
| Power Waste Heat | **ICE, A, B-open** | **80-100 °C cooling system**<br>**400-900 °C Exhaust gas** |
| | **GT, A,B-open** | **250-550 °C** |
| Geothermal | **B-open** | **80-180 °C** |
| Solar Collector | **B-closed** | **<300 °C** |
| Solar pond | **A** | **80-90 °C** |
| Biomass | **B-closed** | **Around 300 °C** |

Open and close types are displayed below.

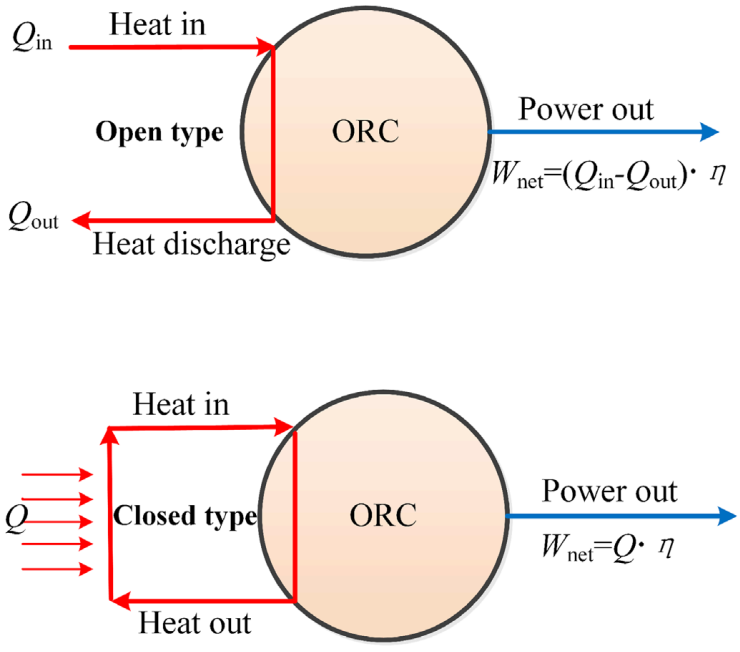


**Figure 2.4:** Schematic diagram of open and closed type heat sources **[2]**.

In table 2.2, locations, flow rates, mean and maximum temperatures of major geothermal resources of Turkey are presented. From the twenty locations seven of them have mean temperatures below 100 C. Ten of them are between 100 and 200 C and three of them are above 200 C. Temperature of 125 C seems to be acceptable considering small drop in temperature from the start point of the source and at the reception point of our ORC system.

**Table 2.2:** Geothermal Energy Potential in Turkey **[21]**.

| **Locality** | **Flow rate (l/s)** | **Ave. Temp(°C)** | **Max. Temp(°C)** |
|---|---|---|---|
| **Germencik/Aydin** | 1515 | 220 | 232 |
| **Sultanhisar-Salavatli/Aydin** | 731 | 163 | 171 |
| **Imamkoy/Aydin** | 40 | 142 | |
| **Omer-Gecek/Afyon** | 817.5 | 94 | |
| **Kizildere/Denizli** | 250 | 217 | 242 |
| **Simav/Kutahya** | 476 | 184 | |
| **Balcova/Izmir** | 536 | 81 | |
| **Seferihisar/Izmir** | 264 | 144 | 153 |
| **Diyadin/Agri** | 561 | 72 | |
| **Sandikli/Afyon** | 496 | 68 | |
| **Dikili/izmir** | 250 | 120 | |
| **Terme/Kirsehir** | 688 | 102 | |
| **Kozakli/Nevsehir** | 247 | 91 | |
| **Golemezli/Denizli** | 340 | 70 | |
| **Kuzuluk/Sakarya** | 271 | 81 | |
| **Tuzla/Canakkale** | 120 | 160 | 174 |
| **Kula/Manisa** | 140 | 135 | |
| **Salihli/Manisa** | 150 | 104 | |
| **Caferbeyli/Manisa** | 6.5 | 155 | |
| **Kavaklidere/Manisa** | 6.5 | 215 | |

Heat sink condition is restricted to the environment of the country, which can be different for various locations. Therefore, average ambient temperature based on the

weather reports for Turkey can be considered as 28 C and water temperature of 25 C [22] and can be used at most of the locations in the country.
To avoid thermal pollution to water resources cooling tower for the rejection of the heat to the atmosphere is required.

## 2.4 Organic Fluids

Organic fluids used in ORCs can have various types from some of hydrocarbons to different refrigerants. Following criterion may be taken into measure in choosing a working fluid for ORC:

- More power output and higher efficiency shall be achievable comparing other organic fluids
- High thermal stability and low flammability
- Matter of lower cost and more availability
- Low GWP and ODP
- Low toxicity
- Low corrosion
- Rather high evaporation temperature and melting point
- Higher latent heat for better heat recovery
- High thermal conductivity and better match with heat source temperature to have better heat transfer

### 2.4.1 T-s diagram of major organic fluids and water for comparison

Fig. 11 shows the T–s diagram the saturation curves of water and of a few typical organic fluids used in ORC applications. Categorization of dry, wet and isentropic fluids is based on their slope in T-s diagram. If the slope is negative, the fluid is called wet, because the expansion is likely to fall in two-phase (wet) such as water. If the slop is infinite, the fluid is isentropic. If the slope is positive like R245fa, the fluid is called dry because expansion fall into dry region. For dry organic fluid, the restriction of the steam quality at the end of the expansion process vanishes in an ORC cycle. The entropy difference between saturated liquid and saturated vapor is much smaller for organic fluids. Hence, the vaporization enthalpy is smaller. Therefore, to absorb equal

thermal energy in the evaporator, the organic working fluid mass flow rate must be higher than for water, which results in higher pump consumption [23].

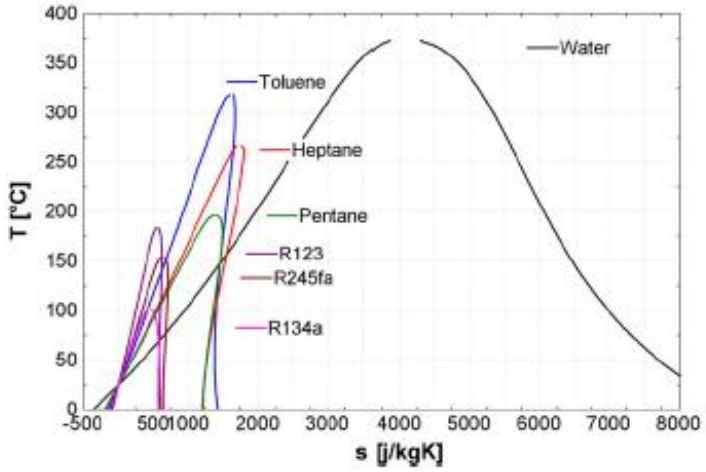


**Figure 2.5:** T-s Diagram of major organic fluids and water **[23]**.

In table 2.3, physical and environmental data of the main organic fluids are encapsulated. A few of the fluids can be suitable considering the criterions mentioned earlier for using in ORC system such as R245fa, R601, R141b, and R123, which have acceptable boiling temperature and density, however R601 has some safety issues like high flammability and R141b, and R123 have rather higher GWP and ODP. Considering all of criterions, R-245fa seems to be suitable and reliable fluid especially because of physical properties, safety and environmental matters (safety datasheet link in references) [24]. R-245fa fluid also widely used by the famous companies producing ORC power boxes.

**Table 2.3:** Physical, safety and environmental data of typical ORC fluids **[10]**.

| Hydrofluorocarbons (HFCs) | Physical data * | | | | Standard 34 * Safety group | Environmental data * | | |
|---|---|---|---|---|---|---|---|---|
| | M [g/mol] | $T_b$ [C] | Tcrit [C] | Pcrit [kPa] | | GWP 100 yr | ODP | Atm. life (yr) |
| HFC-245fa (R245fa) | 134.05 | 15.14 | 154.01 | 3651.0 | B1 | 1050 | 0.000 | 7.7 |
| HFC-236fa (R236fa) | 152.04 | -1.44 | 124.92 | 3200.0 | A1 | 9820 | 0.000 | 242 |
| HFC-152a (R152a) | 66.051 | -24.023 | 113.26 | 4516.8 | A2 | 133 | 0.000 | 1.5 |
| HFC-227ea (R227ea) | 170.03 | -16.34 | 101.75 | 2925.0 | A1 | 3580 | 0.000 | 38.9 |
| HFC-134a (R134a) | 102.03 | -26.074 | 101.06 | 4059.3 | A1 | 1370 | 0.000 | 13.4 |
| HFC-32 (R32) | 52.024 | -51.651 | 78.105 | 5782.0 | A2L r | 716 | 0.000 | 5.2 |
| HFC-143a (R143a) | 84.041 | -47.241 | 72.707 | 3761.0 | A2L r | 4180 | 0.000 | 47.1 |
| HFC-125 (R125) | 120.02 | -48.09 | 66.023 | 3617.7 | A1 | 3420 | 0.000 | 28.2 |
| Hydrocarbons (HCs) | Physical data * | | | | Standard 34 Safety group | Environmental data | | |
| | M [g/mol] | $T_b$ [C] | Tcrit [C] | Pcrit [kPa] | | GWP 100 yr | ODP | Atm. life (yr) |
| n-Pentane (R-601) | 72.149 | 36.06 | 196.55 | 3370.0 | A3 | ~20 | 0.000 | 0.009 |
| n-butane (R-600) | 58.122 | -0.49 | 151.98 | 3796.0 | A3 | ~20 | 0.000 | 0.018 |
| Iso-butane (R-600a) | 58.122 | -11.749 | 134.66 | 3629.0 | A3 | ~20 | 0.000 | 0.016 |
| Propane (R-290) | 44.096 | -42.114 | 96.74 | 4251.2 | A3 | ~20 | 0.000 | 0.041 |
| Hydrochoroflurocarbons (HCFCs) | Physical data * | | | | Standard 34 Safety group | Environmental data | | |
| | M [g/mol] | $T_b$ [C] | Tcrit [C] | Pcrit [kPa] | | GWP 100 yr | ODP | Atm. life (yr) |
| HCFC-141b (R141b) | 116.95 | 32.05 | 204.35 | 4212.0 | n.a. | 717 | 0.120 | 9.2 |
| HCFC-123 (R123) | 152.93 | 27.823 | 183.68 | 3661.8 | B1 | 77 | 0.010 | 1.3 |
| HCFC-142b (R142b) | 100.5 | -9.12 | 137.11 | 4055.0 | A2 | 2220 | 0.060 | 17.2 |
| HCFC-124 (R124) | 136.48 | -11.963 | 122.28 | 3624.3 | A1 | 619 | 0.020 | 5.9 |
| HCFC-22 (R22) | 86.468 | -40.81 | 96.145 | 4990.0 | A1 | 1790 | 0.040 | 11.9 |
| HFO-1234ze (E) | 114.04 | -18.95 | 109.37 | 3636.3 | n.a. | 6 | 0.000 | 0.045 |
| HFO-1234yf (R1234yf) | 114.04 | -29.45 | 94.7 | 3382.2 | A2L r | < 4.4 | 0.000 | 0.029 |
| Ammonia (R-717) | 17.03 | -33.327 | 132.25 | 11333.0 | B2L r | < 1 | 0.000 | < 0.02 |

*: physical properties of working fluids are calculated by REFPROP 9.0 (Eric 2012)
*: (Calm and Hourahan 2011)

## 2.5 Heat Exchangers

Heat exchangers in ORC units are the vital part of the unit. In evaporator a fluid usually passes three processes which are single phase heat addition in preheat evaporation and superheat region (HEX dependent) and in the condenser, single phase heat rejection in desuperheat, condensation and subcool region(HEX dependent). With use of recuperator in some ORC designs, need for preheat and desuperheat process may be lower.

### 2.5.1 Common heat exchangers in ORC modules

Shell-and-Tube, air-cooled and plate (Brazed and Gasketed) Heat Exchangers are the most common and widely used exchangers in ORC systems. Any of these heat exchangers is utilizable depending on the heat source fluid, which can be liquid, or gas and the capacity of the heat exchanger. PHE is chosen because our heat source and heat sink fluids are selected as liquid. So we choose PHE as our evaporator (consist of preheater, evporator and superheater) and condenser (consist of desuperheater and condenser).

*Plate Heat Exchanger*

The plate heat exchanger (PHE) is a suitable type of equipment for heat transfer between liquid flows. In the order of resistance to leakage, there are three types of PHEs, welded as the most resistant to leakage, brazed that have less resistance to leakage than welded, and gasketed which is least resistant comparing other two. PHE has multiple advantages like compactness of the device, high heat transfer coefficients, lower pressure drop, counter-flow regime capability, small end temperature differences, single or multi pass configuration capability, low liquid delay capability, and low fouling. Mainly it consists of a large quantity of parallel stamped or carved rectangular thin metal plates with well-suited corrugations both to increase turbulence in the flow regime and to enable the formation of channels between plates. To address other advantages of a gasketed PHE, ease of disassembling for maintenance, cleaning and adjustment of the number of plates (in the same frame in order to meet other requirements than from the designed) can be mentioned. In the presence of gaskets in the gasketed types, there are some limitations for example the maximum working pressure is usually limited to 10-16 bars (In some cases special construction can double this amount). Regarding operation area of these three types, gasketed plates are preferred in industrial heat exchangers where flexibility is vital to operations, welded types are rare because of increased cost but brazed plate heat exchangers are common in HVAC sector where replacement is easier. Geometrical characteristics of a plate in PHE presented in Figure 12. Flow configuration in plate HEX is depicted in Figure 13.

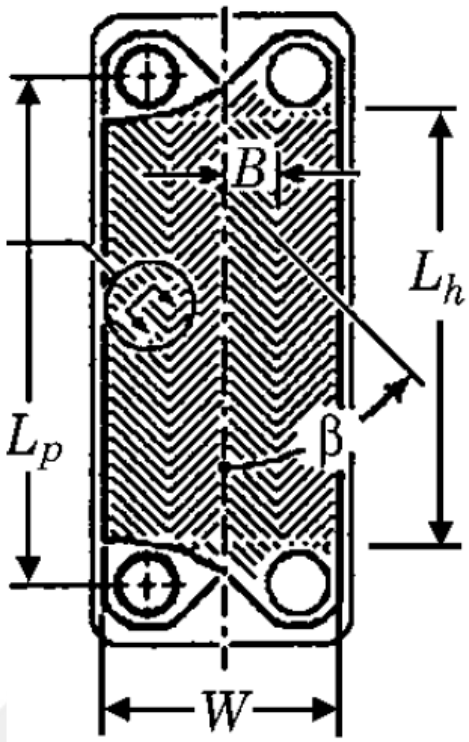


**Figure 2.6:** PHE Plate characteristics **[25]**.

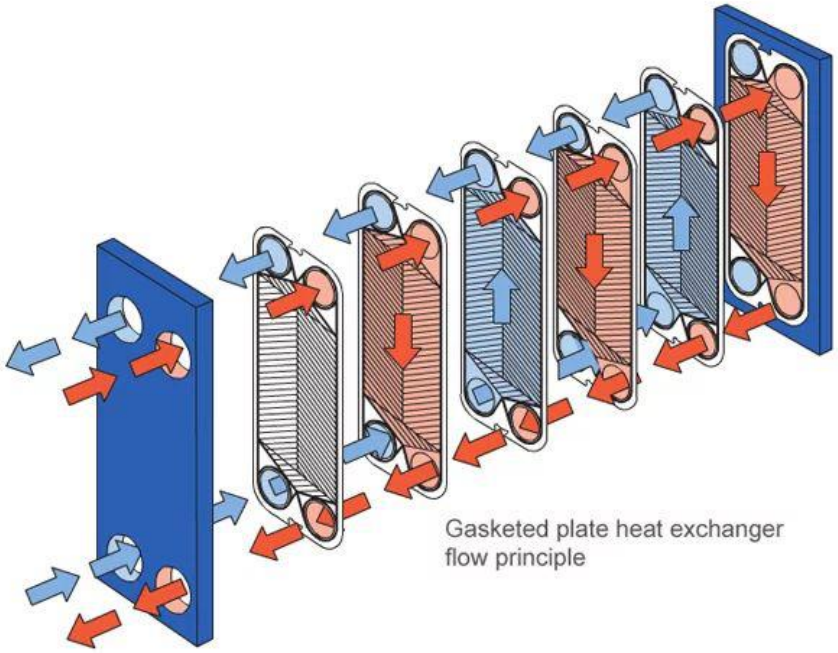


**Figure 2.7:** Flow configuration in plate heat exchanger **[26]**.

### 2.5.2 Ɛ-NTU method

In this method, three dimensionless numbers implemented to calculate the actual transferred heat in a heat exchanger. Ɛ, NTU, $C^*$ definitions are illustrated next.

*U parameter*

Overall Heat transfer coefficient can be calculated as follow.

$$\frac{1}{UA} = \frac{1}{A_c}\left(\frac{1}{h_c} + R_c + \left(\frac{\delta}{k}\right)_{wall} + \frac{1}{h_h} + R_h\right) \tag{2.1}$$

*Number of transfer units (NTU) parameter*

NTU parameter formula is as follows:

$$NTU = \frac{UA}{(\dot{m}C_p)_{min}} \tag{2.2}$$

*Heat capacity rate ratio ($C^*$) Parameter*

$C^*$ parameter can be calculated as follows:

$$C^* = \frac{C_{min}}{C_{max}} = \frac{(\dot{m}C_p)_{min}}{(\dot{m}C_p)_{max}} \tag{2.3}$$

*Heat exchanger effectiveness (Ɛ) parameter*

The Ɛ parameter is non-dimensional and is dependent on the number of transfer units (NTU), the heat capacity ratio $C^*$ and the flow arrangement for a direct-transfer type heat exchanger:

Ɛ=Φ(NTU, $C^*$, flow arrangement)

With considering counter flow as our flow arrangement, effectiveness can be formulated as follows:

$$\varepsilon = \frac{1 - \exp[-NTU(1 - C^*)]}{1 - \exp C^*[-NTU(1 - C^*)]} \tag{2.4}$$

For the case of evaporation or condensation $C^*$(refrigerant side is $C_{max} = \infty$) becomes zero and effectiveness formula becomes:

$$\varepsilon = 1 - \exp(-NTU) \tag{2.5}$$

*Maximum heat transfer $q_{max}$ and heat transfer q*

Maximum heat transfer formula based on cold and hot side inlet temperature is as follows:

$$q_{max} = C_{min}(T_{h,i} - T_{c,i}) \tag{2.6}$$

In addition, since transferred heat formula is:

$$q = \varepsilon q_{max} \tag{2.7}$$

So the transferred heat formula can be illustrated as:

$$q = \varepsilon . C_{min}(T_{h,i} - T_{c,i}) \tag{2.8}$$

In which Ɛ is the exchanger effectiveness, $C_{min}$ is the minimum of $C_h$ and $C_c$, and $\Delta T_{max}=T_{h,i}-T_{c,I}$ which is defined as inlet temperature difference (ITD).

### 2.5.3 Heat and flow Equations used for single phase heat transfer

Martin (1996) proposes comprehensive correlations for friction factors and Nusselt numbers for PHE geometry. The correlation for friction factor is valid for the corrugation angle (β) within 0 to 80 and is accurate within -50% and +100%. Of course, this correlation can be enhanced further if the real detailed geometrical information would be available. Martin (1996) also obtained the Nusselt number correlation as follows, using the momentum and heat transfer analogy from a generalized Le´veˆque solution in thermal entrance turbulent flow in a circular pipe (Schlünder, 1998) [25]:

$$f_0 = \frac{16}{Re} \quad if \;\; Re < 2000 \tag{2.9}$$

$$f_0 = (1.56.\ln(Re) - 3)^{-2} \quad if \;\; Re \geq 2000 \tag{2.10}$$

$$f_1 = (0.9625 + \frac{149.25}{Re} \quad if \ \ Re < 2000 \tag{2.11}$$

$$f_1 = \frac{9.75}{Re^{0.289}} \quad if \ \ Re \geq 2000 \tag{2.12}$$

$$f = [\frac{1 - \cos(\beta)}{(3.8.f_{.1})^{0.5}} + \frac{\cos(\beta)}{(0.045.\tan\beta + 0.09.\sin(\beta) + \frac{f_{.0}}{\cos(\beta)})^{0.5}}]^{-2} \tag{2.13}$$

$$Nu = 0.205Pr^{\frac{1}{3}}.(\frac{\mu}{\mu_{.wall}})^{\frac{1}{6}}.(f.Re^2.\sin(2\beta)^{0.374} \tag{2.14}$$

$$Re = \frac{G.D_e}{\mu}, Pr = \frac{\mu.C_p}{k}, D_e = \frac{2a}{\phi}, G = \frac{\dot{m}}{A_o}$$

$f_0$ and $f_1$ are the limiting friction coefficients in case of $\beta = 0°$ and $\beta = 90°$

### 2.5.4 Heat and flow equations in plate evaporators and Condensers

Suitable correlations are necessary to calculate transferred actual heat and pressure drop in evaporators and condensers. In the case of our ORC system and operating condition, following correlations for evaporation and condensation process that are obtained from experimental studies are suggested.

*Equations of heat transfer correlation for evaporator*

For boiling process in evaporator, Muhammad Imran and his friends (2017) presents the following correlations that obtained by adopting multivariate regression approach [11].

For 45-degree chevron angle:

$$Nu_{boil} = 3.61.{Re_{ref}}^{2.384}.{We_m}^{-0.229}.Bd^{-0.76}.{Bo_{eq}}^{1.321} \tag{2.15}$$

For 60-degree chevron angle:

$$Nu_{boil} = 5.89.{Re_{ref}}^{2.905}.{We_m}^{-0.6087}.Bd^{-0.985}.{Bo_{eq}}^{1.568} \tag{2.16}$$

*Pressure drop in evaporator*

The total pressure drop across brazed plate evaporator of an ORC system consist of four components, among which friction pressure drop is the largest component of pressure drop. Frictional pressure drop consist of 90% of the total pressure drop in the brazed plate evaporator of ORC system and the calculation of the port pipe pressure drop shows that its contribution in total pressure drop is less than 0.5%. Therefore, this pressure drop component is neglected in the pressure drop calculation [11].

For fanning friction factor, following correlations proposed again by Muhammad Imran and his friends (2017).

For 45-degree chevron angle:

$$f_{boil} = 1.37.{Re_{ref_{eq}}}^{-0.0611}.{We_m}^{-0.64}.Bd^{0.0375}.{Bo_{eq}}^{0.045} \tag{2.17}$$

For 60-degree chevron angle:

$$f_{boil} = 2.57.{Re_{ref_{eq}}}^{-0.246}.{We_m}^{-0.3716}.Bd^{0.0815}.{Bo_{eq}}^{1.568} \tag{2.18}$$

$$\rho_m = (\frac{x}{\rho_v} + \frac{1-x}{\rho_l})^{-1} \tag{2.19}$$

$$\Delta P_{Boil} = \frac{f_{Boil}.L.G.N_t}{2.\rho_m.D_h} \tag{2.20}$$

$$We_m = \frac{\rho_m V^2 D_e}{\sigma}, Bo_{eq} = \frac{q}{Gh_{fg}}, Bd = \frac{9.81{D_e}^2(\rho_l - \rho_v)}{\sigma}$$

$$Nu_{boil} = \frac{hD_h}{k}$$

*Equations of heat transfer correlation for condenser*

For condensation, correlations developed by Mancin et al are used. These correlations are implemented by Xianglong Luo and his friends (2017) for pure and mixtures of R245fa condensation in PHE [12].

$$h_A = h_l.[1 + 1.128.x^{0.817}.\left(\frac{\rho_l}{\rho_v}\right)^{0.3685}.\left(\frac{\mu_l}{\mu_v}\right)^{0.2263}.\left(1 - \frac{\mu_v}{\mu_l}\right)^{2.144}.Pr^{-0.1} \tag{2.21}$$

$$h_{Nu} = 0.943.\left[\frac{\rho_l.(\rho_l - \rho_v).9.81.h_{fg}.k^3}{\mu_l.L.(T - T_w)}\right]^{0.25} \quad (2.22)$$

$$h_c = ({h_A}^2 + {h_{Nu}}^2)^{0.5} \quad (2.23)$$

$$h_{tp} = h_c.[1.074.(T_{sat} - T_w)^{-0.386} \quad (2.24)$$

$h_{Nu}$: Gravity driven condensation

$h_l$:Single phase HTC

$h_A$: Shear dominated mean HTC

$h_c$:Root mean square of $h_A$

$h_{tp}$: Tow phase flow HTC

*Frictional pressure drop in condenser*

The frictional pressure drop correlation presented by Wang et al. is used in the present study. Equations down below provide the frictional pressure drops in the two-phase, liquid phase, and vapor phase [12].

$$f_l = 0.56.{Re_{.ref\_l}}^{-0.12} \quad (2.25)$$

$$f_v = 0.56.{Re_{.ref\_v}}^{-0.12} \quad (2.26)$$

$$\Delta P_l = f_l.\frac{L}{D_h}.\frac{[G_{.c}.(1-x)]^2}{2.\rho_l} \quad (2.27)$$

$$\Delta P_v = f_v.\frac{L}{D_h}.\frac{[G_{.c}.(x)]^2}{2.\rho_v} \quad (2.28)$$

$$X = (\frac{\Delta P_l}{\Delta P_v})^{0.5} \quad (2.29)$$

$$\Phi = (1 + \frac{16}{X} + \frac{1}{X^2})^{0.5} \quad (2.30)$$

$$\Delta P_f = \Phi^2.\Delta P_l \quad (2.31)$$

## 2.6 Expander

The expansion machine is one of the four main components of an Organic Rankine Cycle (ORC) system. Performance of the expander can largely affects the whole system. In addition, the expander play a crucial role in the control of the ORC system. In the present chapter, our aim is to introduce briefly the principle of operation of main technologies in displacement expanders, and to mention their advantages, and disadvantages.

### 2.6.1 Definition

A positive displacement or by another word volumetric expander is an expansion device in which as its volume gradually increases, the operating fluid pressure is being decreased. The volumetric expander usually consist of a stator and one or few rotors connected to the shaft of expander. Positions of rotors change depending on angular position of rotating shaft; this defines multiple chambers containing confined fluid. The high-pressure fluid press the rotors to move. Fluid pressure decreases gradually as the volume of the working chambers increases. Transferred Energy by the form of mechanical work, appears in the form of decrease in the fluid energy [28].

The technical aspects and the market of this kind of expanders in ORC systems is very little compared with displacement compressors used in HVAC&R (Heating, Ventilation, Air-Conditioning and Refrigeration) and the compressed air industry. Although some technologies of large-scale displacement expanders have been progressed and commercialized for many years, but there are still many R&D activities in progress to improve displacement expanders that suit the needs of ORC systems. This type of expanders utilized in ORC systems with power lower than 150 kWe [28].

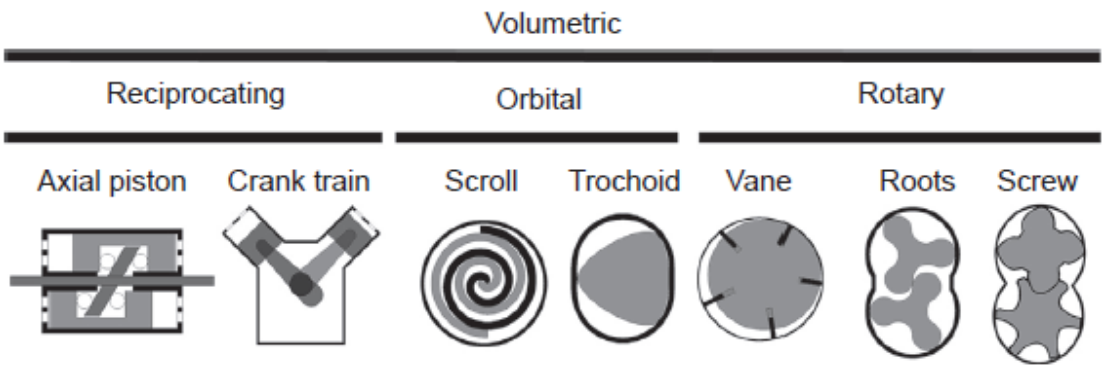


**Figure 2.8:** Different Volumetric Expanders **[27]**.

### 2.6.2 Piston expanders

A reciprocating expander, or piston expander, is consist of one or multiple cylinders. In this type of expander displacement of pistons are in a reciprocating manner from the Top Dead Center (TDC) to the Bottom Dead Center (BDC). Entry and exit of fluid to the cylinder take place through orifices equipped with valves [5].

### 2.6.3 Twin-screw expanders

A twin-screw expander comprises two interlocking screw-shaped toothed rotors (the male and the female rotors) which are placed in a casing. The rotors movement and the casing define multiple working chambers that develop from one end of the rotors to the other one [5].

### 2.6.4 Scroll expanders

Scroll expanders are from the family of orbiting machines. They are consist of two involutes, one placed in the central symmetry of the other. Usually, one involute is stationary the other one, however has an orbiting movement. Their relative position delimits multiple chambers; Most of them having a configuration of crescent-shape, these chambers play roles as suction, expansion or discharge chambers.

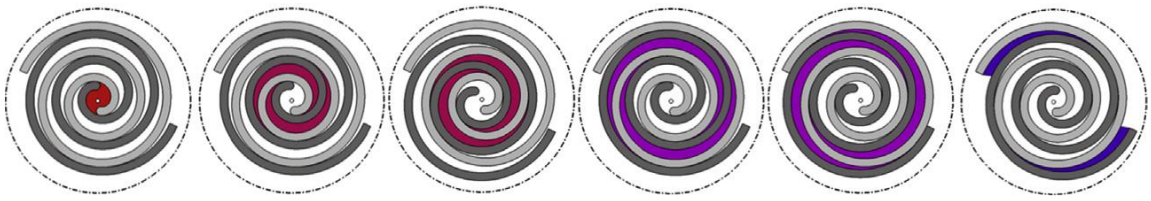

**Figure 2.9:** Schematic of fluid expansion in scroll expander **[27]**.

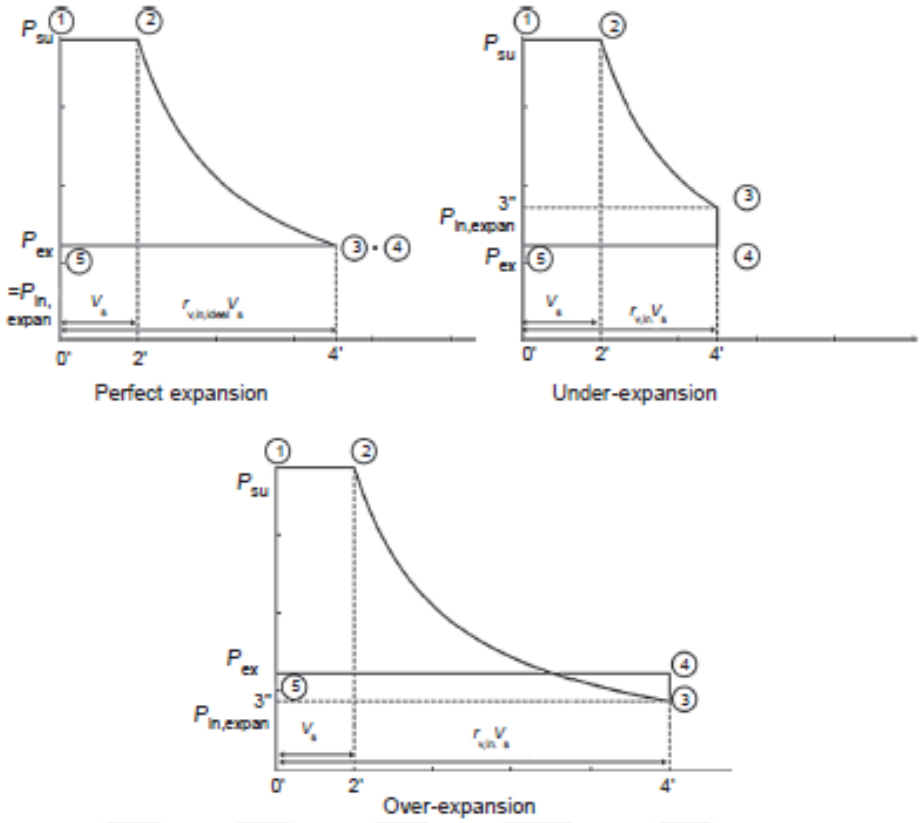


**Figure 2.10:** Theoretical indicator diagram of a scroll expander. Illustration of under-expansion and over-expansion losses **[27]**.

Scroll machines are highly reliable components because of a very low number of ambulant elements. Required maintenance is also low in comparison to most of the expanders. Some scroll machines may need a replacement of a tip seal but most of the time; the machine is designed in a way to require no maintenance at all.

On the other hand, this type of expander has some limitations that we mention them in this section. Scroll expander main limitation is the maximum allowable fluid temperature at the expander supply.

Increased pressure consequently results in higher loads on the bearings of the machine. We suggest this type of expander because of lower rotational speed (which effects positively the lifetime of the expander and better maintenance), less noise and finally medium cost as shown in the Table 2.4 for the low and medium capacities.

**Table 2.4:** Overall comparison of the major expanders **[28]**.

| Expander type | Turbine | Scroll | Screw | Vane | Piston |
|---|---|---|---|---|---|
| Power | High/medium | Medium /low | Medium | Low | Medium |
| Working fluid flow velocity | Very high | Low | Medium | Low | Medium |
| Technical complication | Very high | low | Medium | Low | High |
| Rotational Speed | Very high | Low | low | Low | Medium |
| Noise | High | Low | Medium | Low | High |
| Operation in wet vapor condition | No | No | Yes | Yes | No |
| Difficulty of air-tight sealing | High | Medium | High | Low | High |
| Cost | High | Medium | High | Very low | Medium |
| Service costs | Very high | Medium | High | Very low | Medium |
| Durablity | High | Medium | High | Medium | Medium |
| Internal Mechanical friction | Low | Medium | Medium | Medium | high |

Formula used for power output of the expander:

$$W_{ex} = \dot{m}(h_{inlet} - h_{oulet})\eta_{Expander} \quad (2.32)$$

## 2.7 Pumps in ORC

Pump efficiency can influence the ORC performance to an important extent. Efficient pump can raise the fluid pressure with less power consumption, so less output power of ORC system will be required for pump work.

As a result, right selection for pump is important to acquire desired amount of pressure after the pump. In some cases, special pumps like very accurate double diaphragm

pumps can minimize the leakage; hence, in case of flammable or toxic fluids they are suitable to minimize the leakage and related risks.

Power and formulas related to affinity law are used in our analysis.

$$W_p = \frac{\dot{m}(h_2 - h_1)}{\eta_{pump}} \tag{2.33}$$

$h_2$: Enthalpy of fluid after pump, $h_1$: Enthalpy of fluid before pump

# 3. SIMULATION OF ORC

This chapter is about simulation of our ORC system in Mathcad program, contents of the chapter are briefed as follow.

Subchapter 3.1 is related to schematic diagram of analyzed ORC, and in 3.2 a brief introduction about Mathcad and CoolProp library is made. In 3.3 design conditions in a table are presented and reasons of choosing design parameters are explained, then flowcharts of the procedure of the simulation are explained.

## 3.1 Schematic Diagram of Analyzed ORC System

This ORC system is consist of five main components. Three of them are exchangers, one of them is the evaporator that comprises preheater, evaporator, superheater (theoretically in each of them by order of fluid entry pure preheating ,evaporation and superheating take place), and condenser consist of desuperheater and condenser (theoretically in each of them by the order of entry pure desuperheating ,condensation take place). For expansion process, we have either expansion valve or expander.

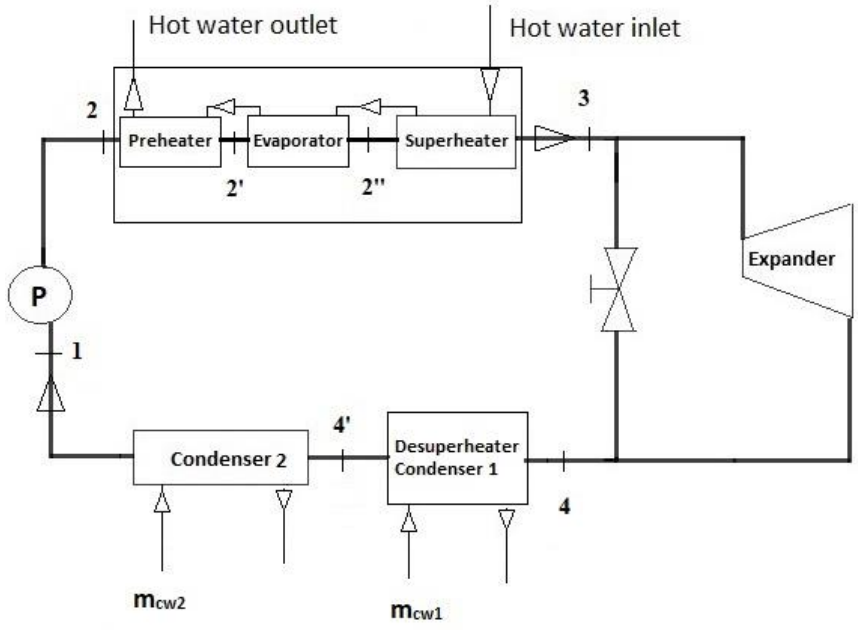


**Figure 3.1:** ORC Schematic

## 3.2 Brief Introduction of Mathcad and CoolProp Library

“Mathcad is computer software primarily intended for the verification, validation, validation, documentation and re-use of engineering calculation” [29].
“The CoolProp library (Bell et al., 2014) is a C-based open-source library of thermo-physical properties that emulates much of the functionality of REFPROP. Additionally, CoolProp has properties of humid air, incompressible fluids, and brines, as well as tabular interpolation (TTSE and bicubic), for both pure fluids and mixtures (from REFPROP)”[5].

## 3.3 Modeling and Simulation of ORC in Design Condition

To model the ORC system, design conditions are needed to be determined. To perform the calculations in Mathcad, CoolProp library is used to obtain thermodynamic properties of the fluid for different points of ORC, expander and pump work formula used to obtain fluid enthalpies at their outlet.

### 3.3.1 Design condition

In order to have realistic model, expander isentropic efficiency is selected based on a report of the department of energy regarding scroll expanders [30] however for the pump, delivered efficiency of CHI 4-50 model of Grundfos brand is selected for the working condition of the cycle.
Parameters used in evaporator calculations, are chosen based on the operating condition in which Muhammad Usman and his friends acquired their correlations for evaporator, which is mass velocity (G) of within 30-40 kg/m2.s, and heat flux of 2-15 $kW/m^2$ and evaporation temperature of around 70°C[11]. Plate dimensions obtained from manufacturers catalogue (Alfalaval) [31] Evaporator is selected from Alfalaval catalogue based on given capacities of the evaporator, and number of plates for evaporator are chosen in a way to have the mass velocity of 30-40 kg/m2.s.
Regarding condenser, condensation temperature selected in a way so there is adequate ITD from the cold water source. Plate number was also chosen in a way to have a mass velocity of 60 kg/m2.s for the working fluid [12].Water mass flow rate in evaporator and condenser were chosen in a way to have turbulent flow regime in the evaporator and condenser for higher HTC.

Fouling factors for water and refrigerant sides are chosen based on the values provided by Hua Tian, Liwen Chang [32]. All of the design parameters of the simulated ORC system listed in the Table 3.1 as follows:

**Table 3.1:** ORC parameters table

| Parameter | value |
|---|---|
| Condenser pressure, $P_1$ (kPa) | 250 |
| Evaporator pressure, $P_3$ (kPa) | 700 |
| Expander inlet temperature, $T_3$ (°C) | 124 |
| Expander isentropic efficiency, [%] | 75 |
| Pump isentropic efficiency,[%] | 35.6 |
| Net power output, $W_{net}$,[KW] | 5 |
| Excessive cooling at condenser outlet, dT, (°C) | 0 |
| Hot water inlet Temperature, (°C) | 125 |
| Cold water inlet Temperature, (°C) | 25 |

Parameters related to the plate geometry and number of plates for each of HEXs and required length for the processes which are obtained iteratively are listed in the following Table 3.2.

**Table 3.2:** HEX parameters

| HEX parameter | value |
|---|---|
| Chevron angle | 45,60 |
| Plate width (m) | 0.112 |
| Plate length (m) | 0.466 |
| Plate spacing (mm) | 2.3 |
| Evaporator plate number | 30 |
| Condenser and desuperheater plate number | 18 |
| Superheater length (m) | 0.3153 |
| Evaporator length (m) | 0.0635 |
| Preheater length (m) | 0.087 |
| Desuperheater length (m) | 0.146 |
| Condenser1 length (m) | 0.32 |

### 3.3.2 Pump

For compression process, a centrifugal pump is suggested from Grundfos brand CHI 4-50 which is a two-stage centrifugal pump with 35.6% efficiency at the design mass flow rate and head. Enthalpy for the outlet of the pump can be calculated by the following formula.

$$h_2 = h_1 + \frac{v_1(P_2 - P_1)}{\eta_p} \tag{3.1}$$

### 3.3.3 Evaporator

Evaporator in general consist of preheater, evaporator and superheater. Heat transfer rate in each of them calculated by the following formulas.

*Theoretical total heat transfer in all (preheater, evaporator, superheater)*

Theoretical heat transfer rate in evaporator as preheater, evaporator, superheater and each heat transfer in each region are separately explained as following:

Total Heat transfer in evaporator: $$Q_E = (h_3 - h_2)m_r \quad (3.5)$$

Heat addition in Superheater: $$Q_S = \big(h_3 - h_g(P_3)\big)m_r \quad (3.6)$$

Heat addition in Pure Evaporation: $$Q_{EE} = \big(h_g(P_3) - h_l(P_3)\big)m_r \quad (3.7)$$

Heat addition in Preheater: $$Q_P = (h_l(P_3) - h_2)m_r \quad (3.8)$$

*HTC and friction factor calculation procedure for superheater*

Following flowchart is the procedure of calculation of HTC for single-phase heat transfer, fanning friction factor and pressure drop value. Since the working fluid is in gas state there is a single difference in calculation of HTC, which is omitting one of the terms in the equation and replaced it with one (chapter 2).

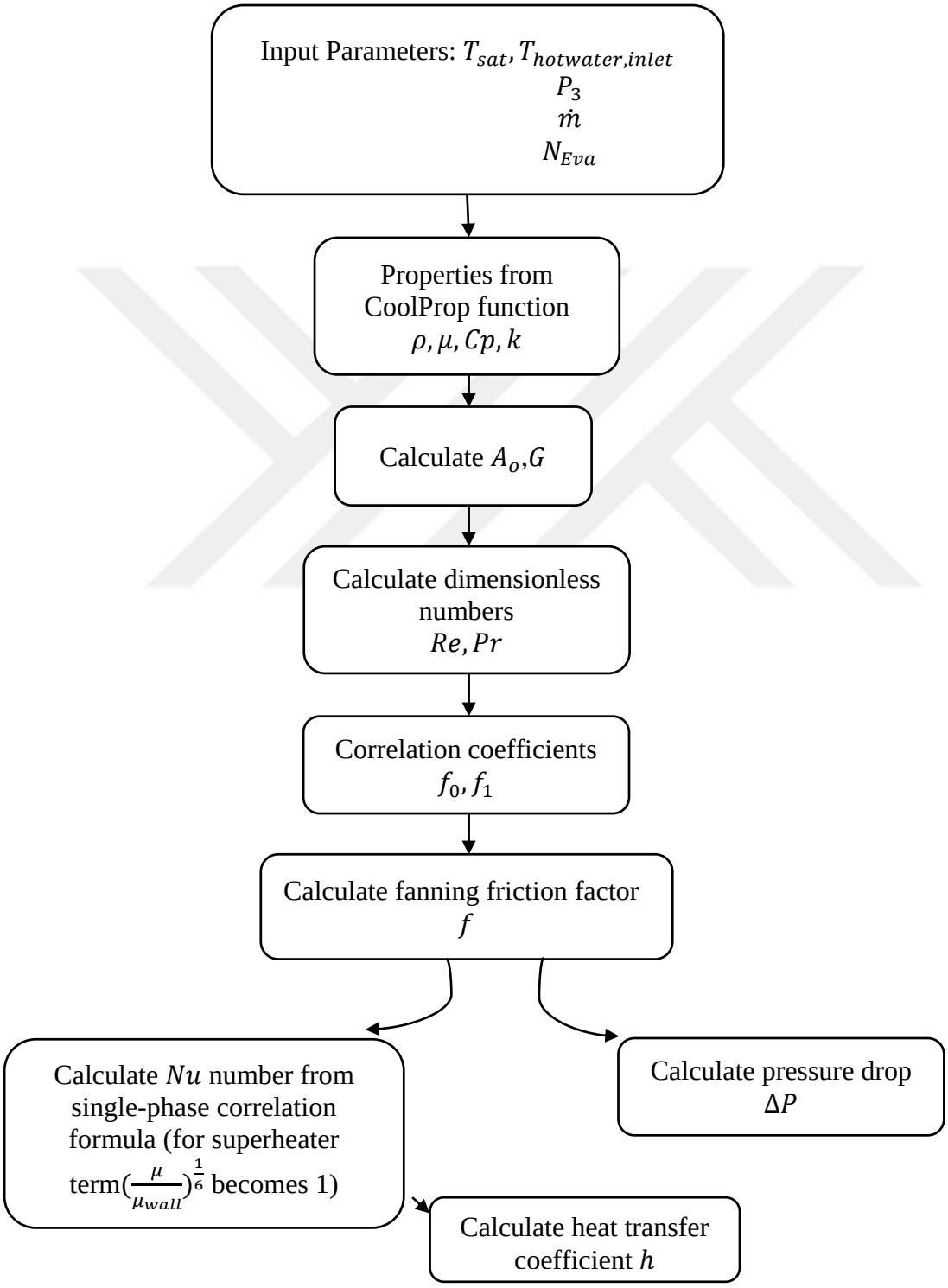


**Figure 3.2:** Flowchart of HTC and friction factor calculation for superheater

*Calculating procedure of U, Ɛ, NTU, q*

Procedure for calculating U, Ɛ, NTU, q is as follows:

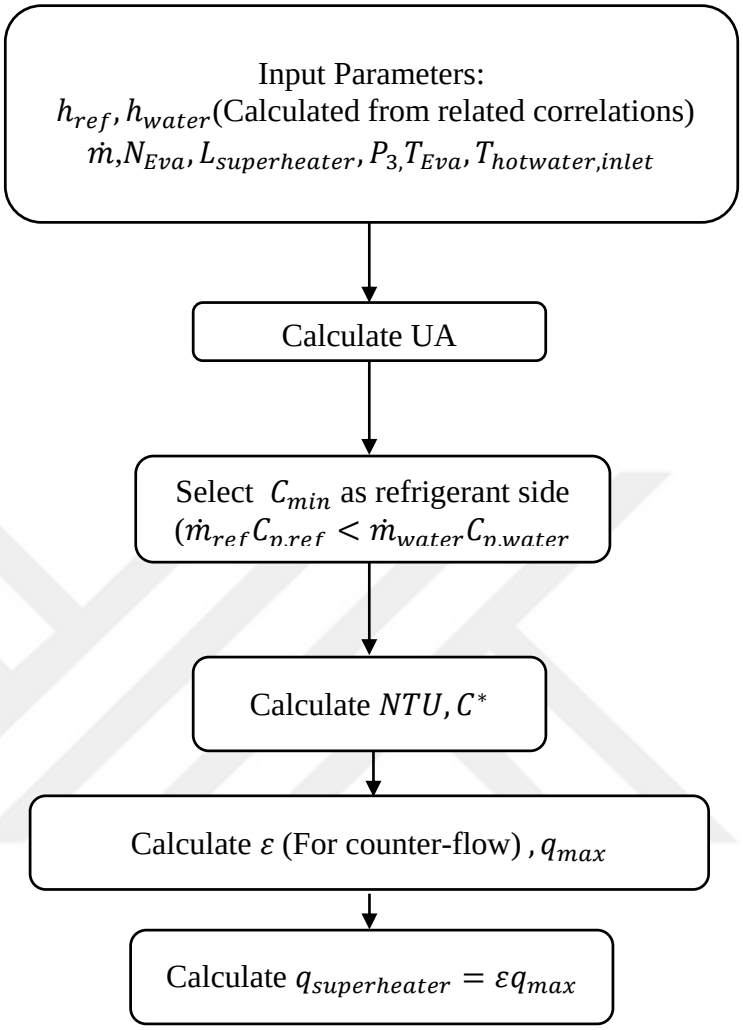


**Figure 3.3:** Flowchart of U, Ɛ, NTU calculation for superheater

*HTC and friction factor calculation procedure for evaporator*

Following flowchart is the procedure of calculating heat transfer coefficient and fanning friction factor and as result pressure drop for evaporator (Pure evaporation). In this procedure, quality (x) is considered as 0.5.

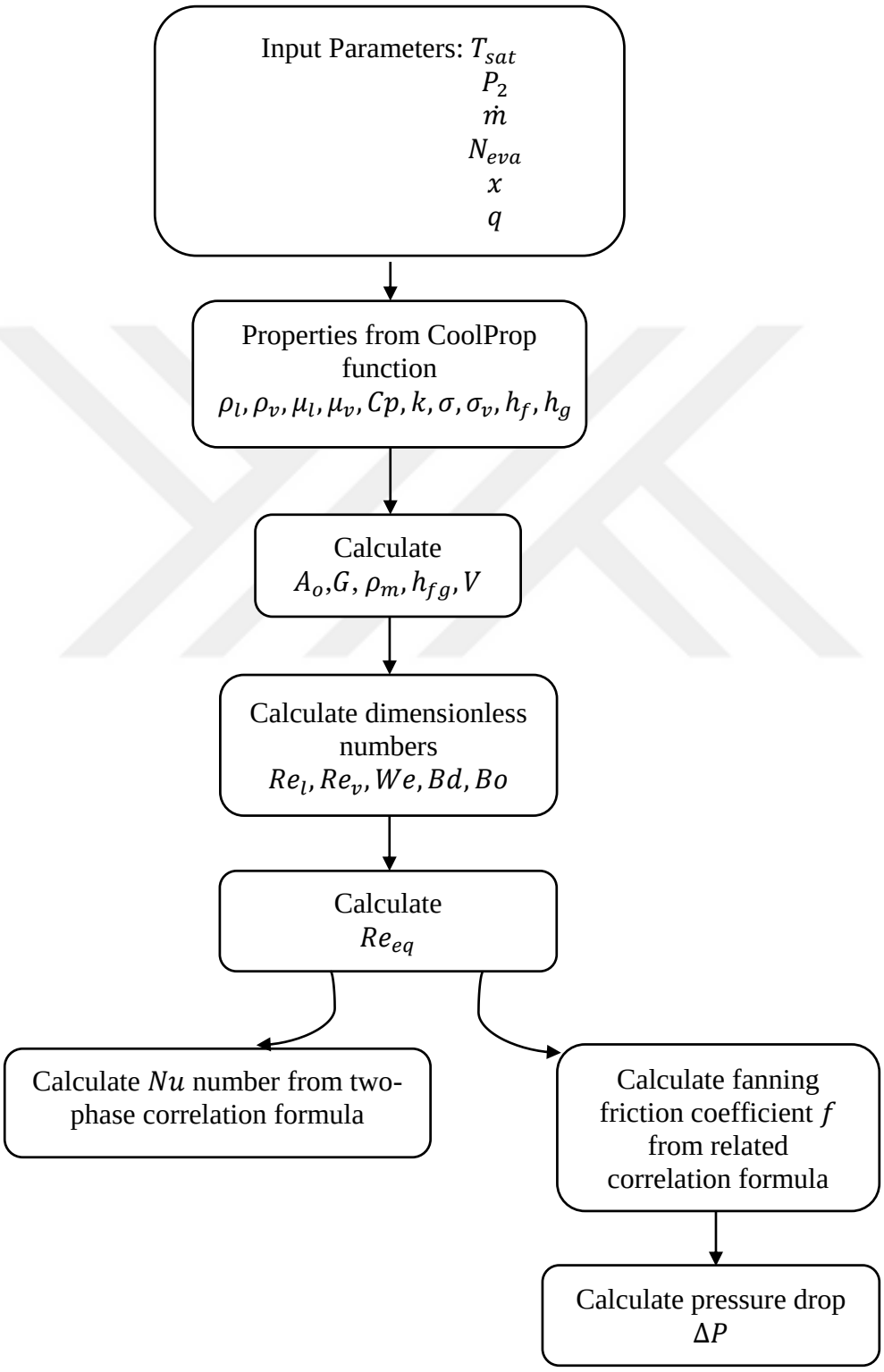


**Figure 3.4:** Flowchart of HTC and friction factor calculation for evaporator

*Calculation of U, Ɛ, NTU, q for evaporator*

Procedure of calculating of U, Ɛ, NTU, q are as follow:

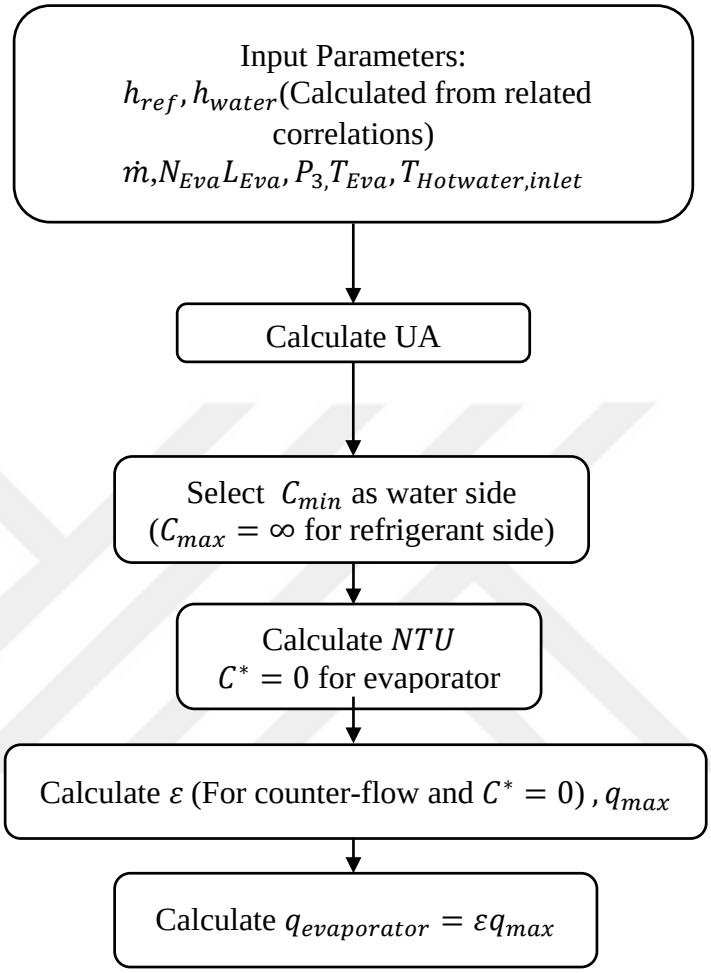


**Figure 3.5:** Flowchart of U, Ɛ, NTU calculation for evaporator

*HTC and friction factor calculation procedure for preheater*

Following flowchart is the procedure of HTC and friction factor and pressure drop calculation for preheater.

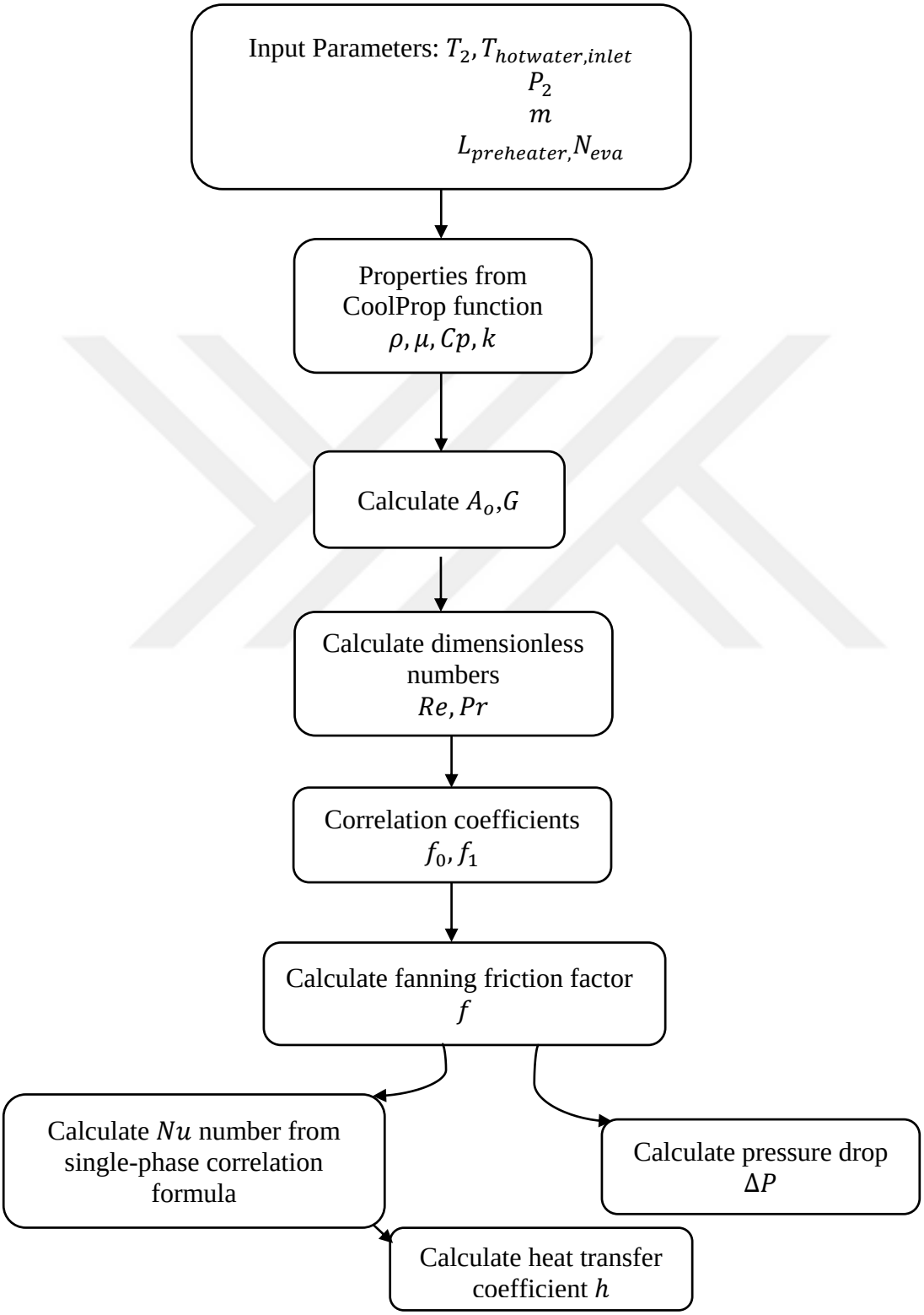


**Figure 3.6:** Flowchart of HTC and friction factor calculation for Preheater

*Calculation of U, Ɛ, NTU, q for preheater*

Procedure for calculating U, Ɛ, NTU, q parameters are the same for superheater.

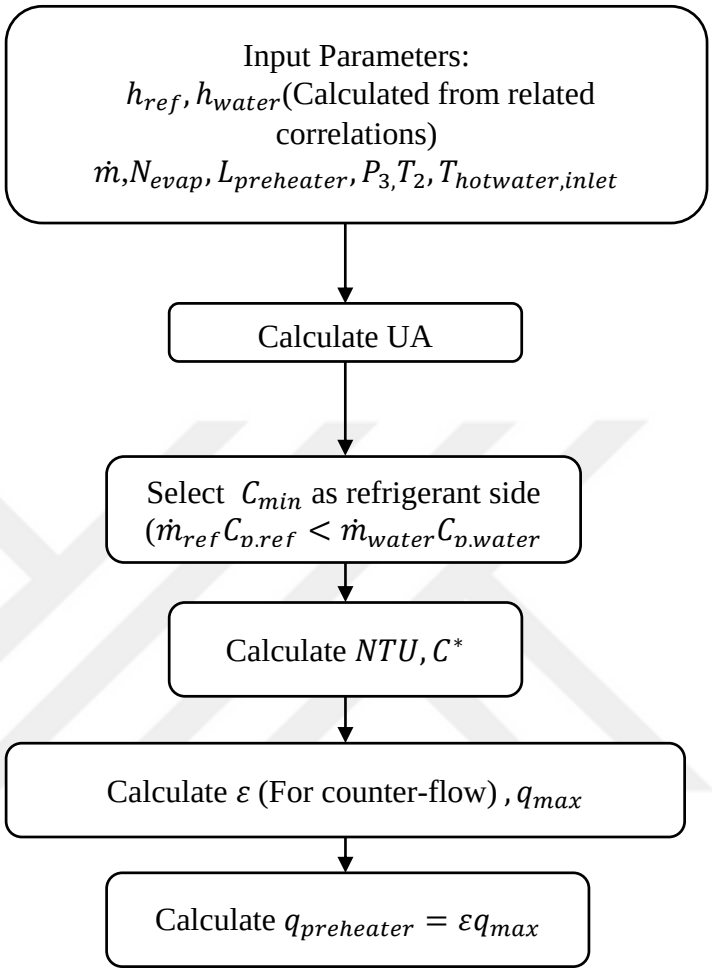


**Figure 3.7:** Flowchart of U, Ɛ, NTU calculation for preheater

### 3.3.4 Condenser

In this section theoretical heat transfer for condenser and obtaining procedure for actual heat transfer and pressure drop equations are discussed.

*Theoretical total heat transfer in all Condenser, Desuperheater*

Theoretical heat transfer in condenser and desuperheater are presented as following. For heat transfer in desuperheater outlet temperature from expander and expansion valve are considered as inlet temperature of desuperheater.

Heat rejection in desuperheater when fluid passes expansion valve and expander:

$$Q_{D1} = \left(h_4 - h_g(P_1)\right)m_r \quad (3.9)$$

$$Q_{D2} = \left(h_3 - h_g(P_1)\right)m_r \quad (3.10)$$

Heat rejection in Pure condensation:

$$Q_{CC} = \left(h_g(P_1) - h_l(P_1)\right)m_r \quad (3.11)$$

*HTC calculation procedure for condenser*

Following flowchart is procedure of calculation of HTC for condenser, in this procedure mean quality (x) is considered 0.5 as in [12].

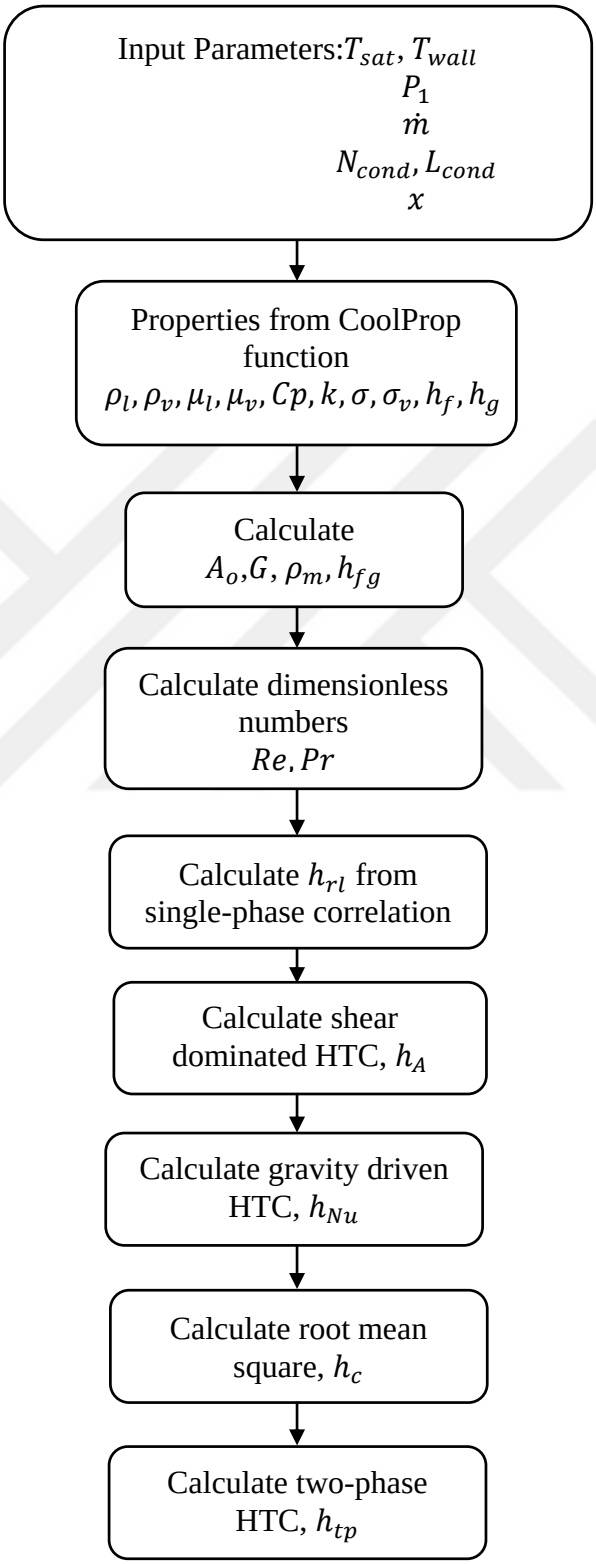


**Figure 3.8:** Flowchart of HTC and friction factor calculation for condenser

*Calculation of U, Ɛ, NTU, q for condenser*

Procedure of calculating of U, Ɛ, NTU, q are as follows, which is similar as evaporator:

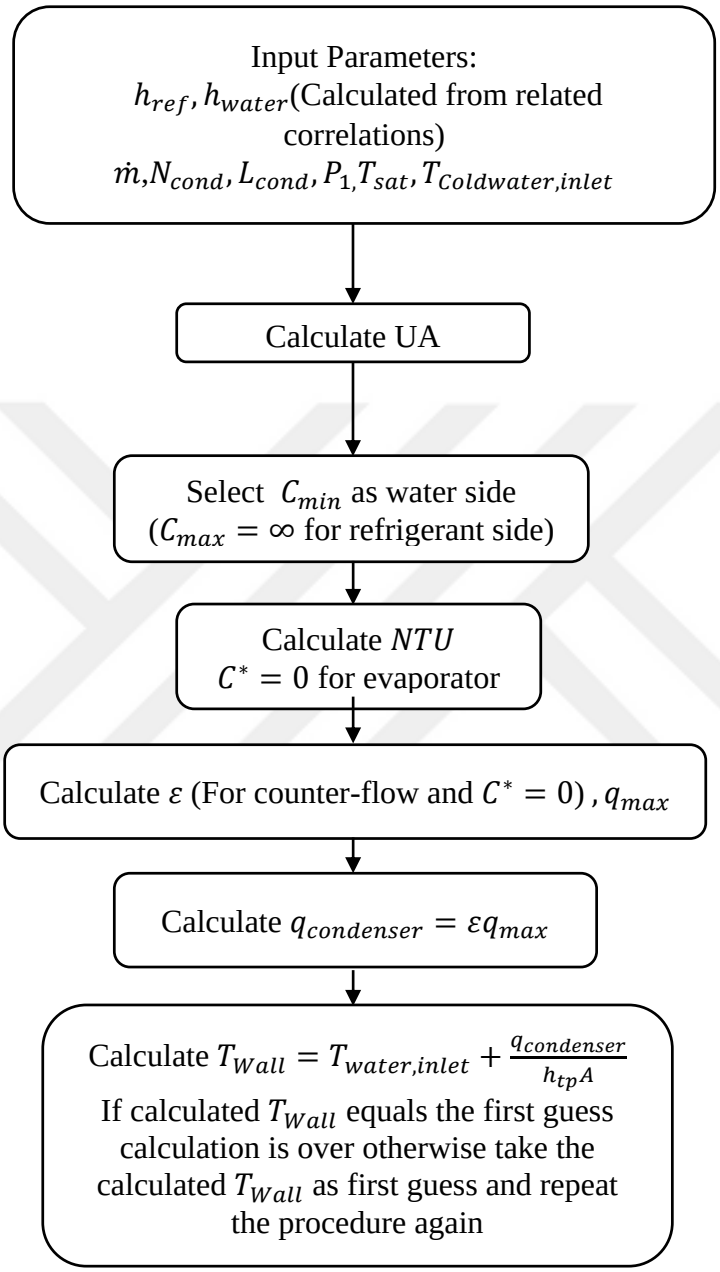


**Figure 3.9:** Flowchart of U, Ɛ, NTU calculation for condenser

*Pressure drop calculation procedure for condenser*

Following flowchart is procedure of calculating Pressure drop for condenser (Pure condensation).

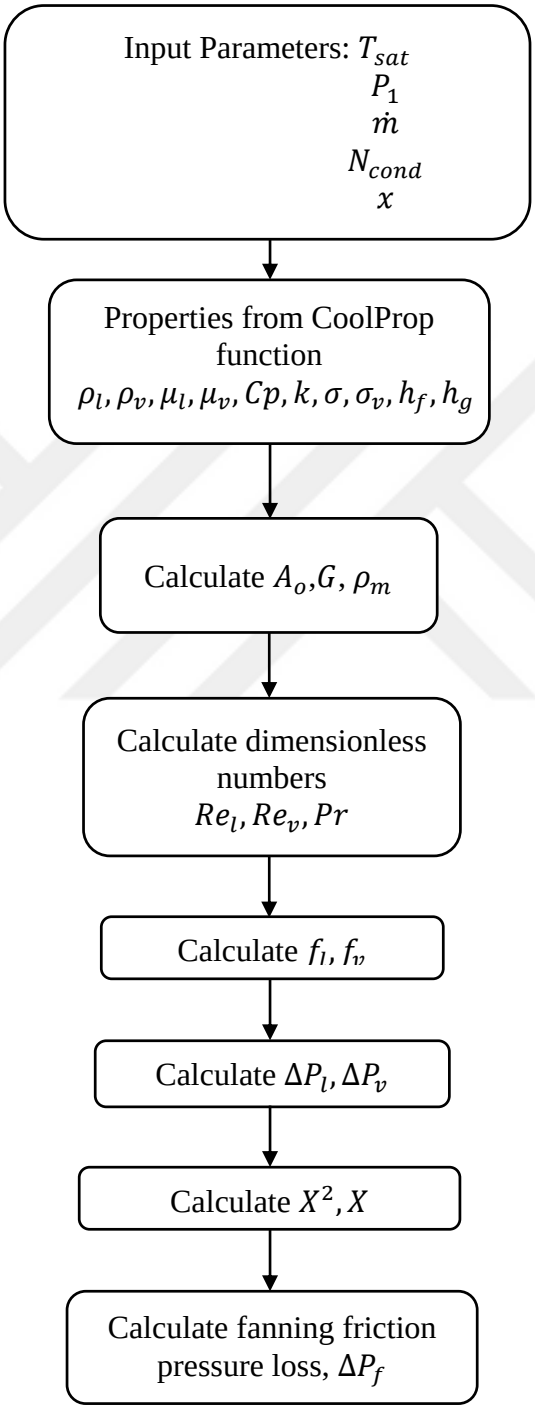


**Figure 3.10:** Flowchart of frictional pressure drop calculation for condenser

*HTC and friction factor calculation procedure for desuperheater*

Following flowchart is procedure of calculation of HTC and friction factor and pressure drop for desuperheater.

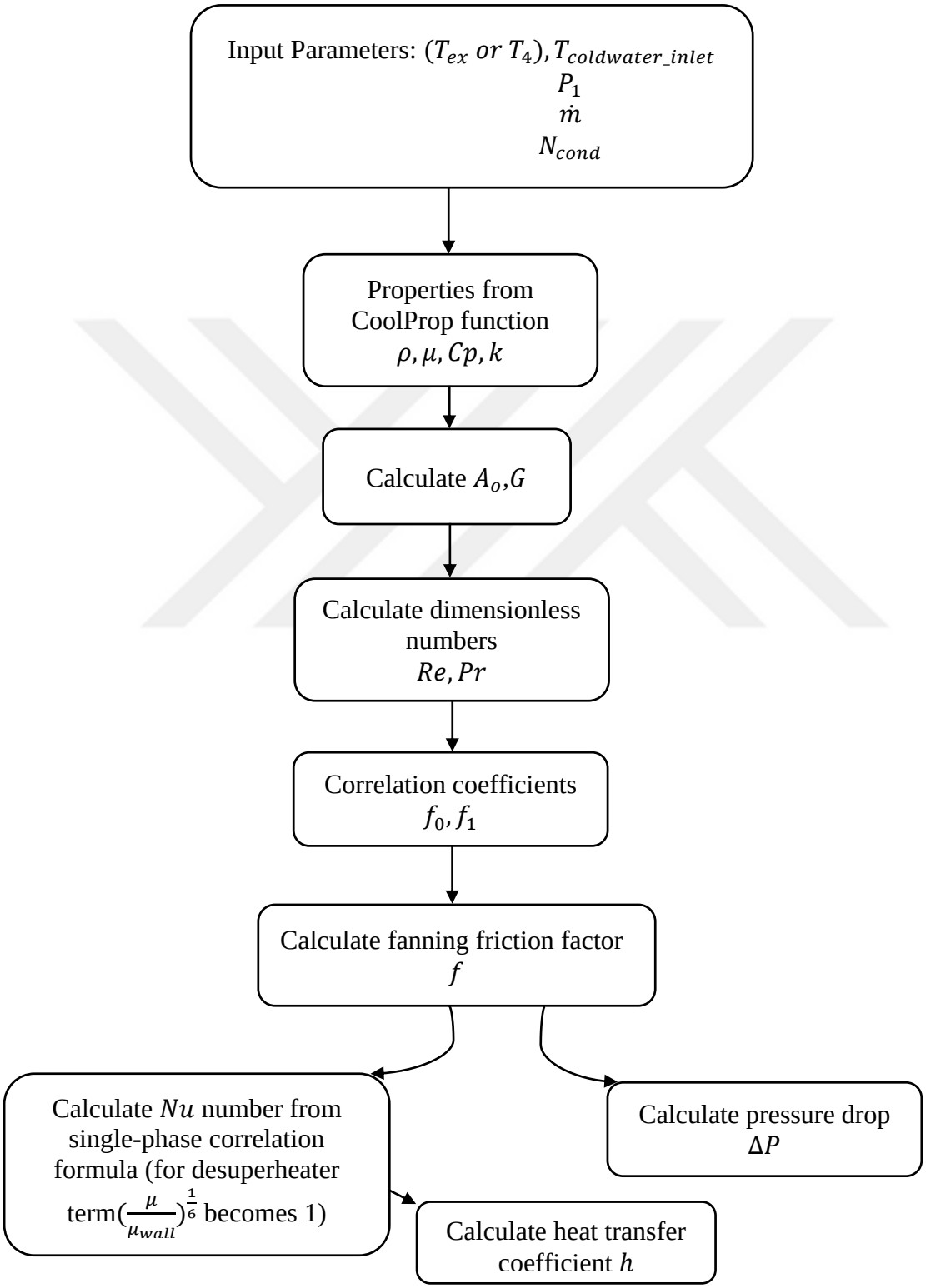


**Figure 3.11:** Flowchart of HTC and friction factor calculation for desuperheater.

*Calculation of U, Ɛ, NTU, q for desuperheater*

Procedure for calculating U, Ɛ, NTU, q parameters is the same as superheater.

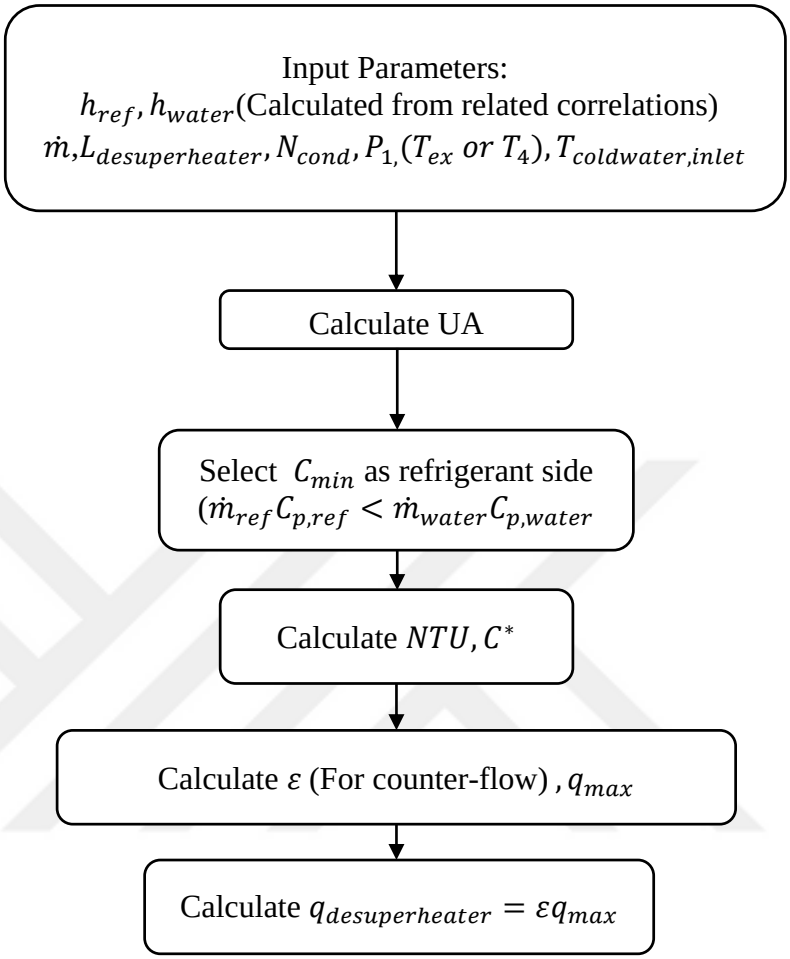


**Figure 3.12:** Flowchart of U, Ɛ, NTU calculation for desuperheater.

### 3.3.5 Expansion valve

Expansion valve is used in real ORC units. Duty of expansion valve is during start-up and shutdowns. In expansion process at expansion valve $h_3 = h_4$. Temperature of point 4 can be calculated by CoolProp function as follows:

$T_{ex}$(P,H):= FluidProp("T", "P", P, "H", H, WFluid)

### 3.3.6 Expander

Theoretical work rate and total work produced by expander can be calculated by the following formulas:

Specific work of expander: $w_{exp} = h_3 - h_4$ (3.8)

Expander Power: $W_{exp} = (h_3 - h_4)m_r$ (3.9)

### 3.3.7 Overall efficiency

Net power and Efficiency definition of cycle follows as:

Net Specific work of cycle: $w_{net} = w_{exp} - w_p$ (3.10)

Thermal efficiency: $\eta_{th} = 1 - \frac{Q_C}{Q_L}$ (3.11)

# 4. RESULTS AND DISCUSSION

Results of the Mathcad program are presented in this chapter. Some comments are also made on the results. Contents of the chapter are briefed as follow.

In this chapter, 4.1 is related to ORC results, the effect of pump and expander efficiencies, condensation and evaporation temperature on the cycle thermal efficiency are scrutinized. Then results of analyzed ORC module are pointed out. In 4.2 which is related to HEX results pressure drop and heat transfer performance of plates with 45 and 60 degrees of chevron angle are investigated. Performance of condenser for both conditions when that fluid passes expander or expansion valve are investigated. Pressure drop results obtained and their effect on pump power is examined. Effect of cold source temperature change on the condenser is also investigated. Finally, to find out optimum area, the effect of evaporation temperature on condenser and evaporator is analyzed.

## 4.1 ORC Results

In this section, results of calculations related to only ORC (HEXs calculations are not accounted in these results) are explained. Diagrams of change of cycle thermal efficiency due to change of pump and expander mechanical efficiency are plotted. To have overview and insight of the ORC, obtained results such as temperature at different points, T-s diagram are mentioned.

### 4.1.1 Pump and expander efficiencies effects on cycle thermal efficiency

To measure the effect of pump efficiency different values for pump efficiency which are between 31 and 81% [33] are tested by keeping other parameters in table 3.1 fixed. Following results are obtained which shows higher efficiency for pump gives higher net power and as a result better cycle thermal efficiency.

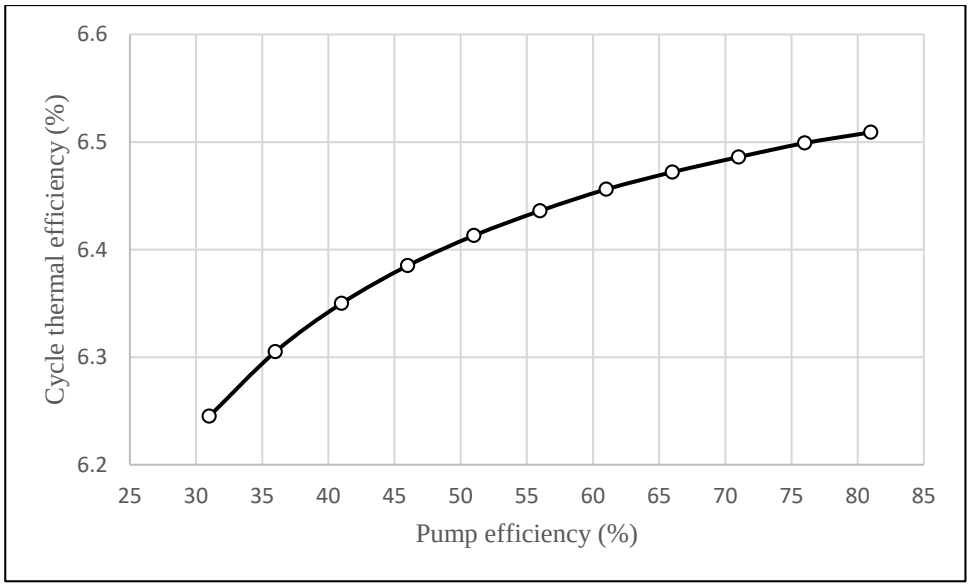


**Figure 4.1:** Pump isentropic efficiency vs cycle thermal efficiency

Regarding scroll expander, mechanical efficiencies between 60 and 76% [34] are tested in the computer program with keeping all of the remaining parameters in table 3.1 fixed. Results show higher expander efficiency can give higher power output and better cycle thermal efficiency.

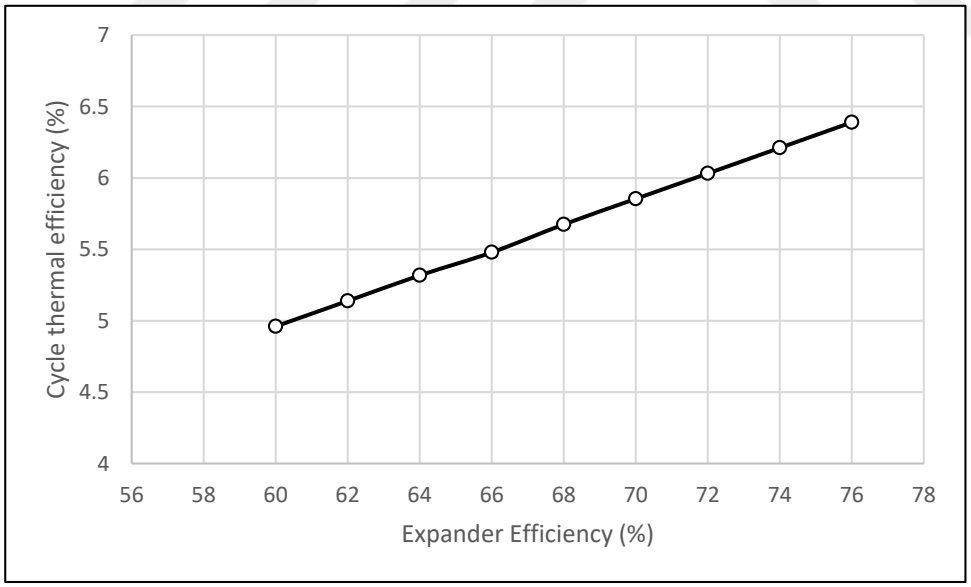


**Figure 4.2:** Expander isentropic efficiency vs cycle thermal efficiency

### 4.1.2 Condensation and evaporation temperatures effects on cycle efficiency

Condensation temperature is related to the outlet pressure of the expander, which depends on expander ratio of inlet, and outlet pressure. In this part, the effect of

condensation pressure is examined with maintaining all other parameters fixed in design parameters table 3.1.

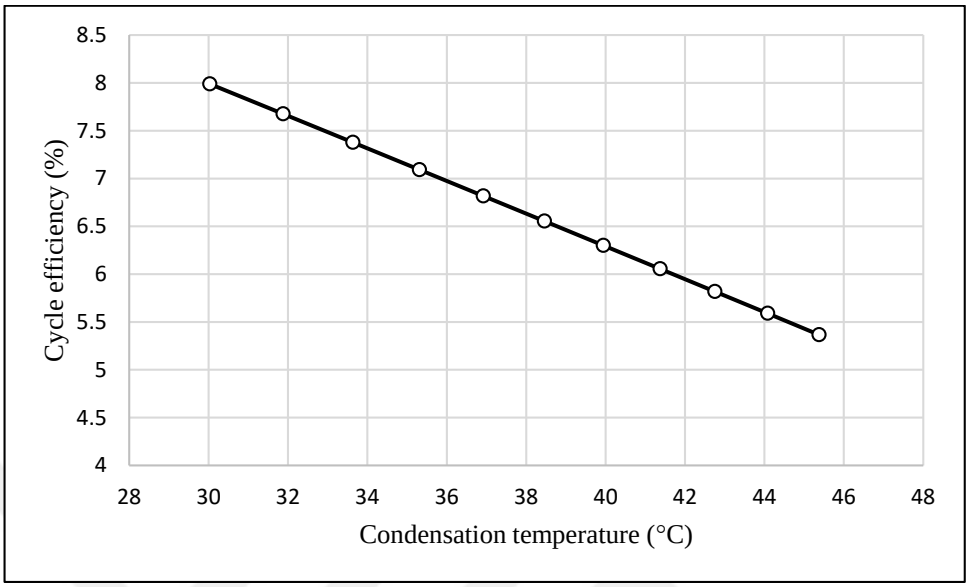


**Figure 4.3:** Condensation temperature vs cycle thermal efficiency

Evaporation temperature is related to the outlet pressure of the pump. In the diagram below the effect of increased evaporation temperature on the thermal efficiency of the cycle is investigated with keeping constant the remaining parameters in table 3.1 .The result shows that by increasing evaporation temperature better cycle thermal efficiency is possible.

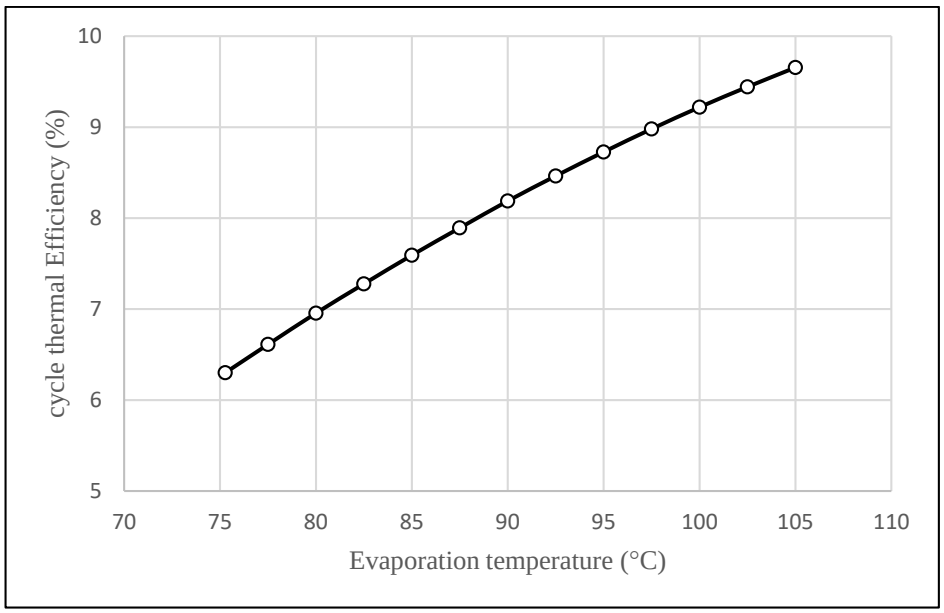


**Figure 4.4:** Evaporation temperature vs cycle thermal efficiency

### 4.1.3 Results of analyzed ORC

Following matrices and T-s diagram are the results obtained from generated computer program with parameters of table 3.1. Mass flow rate, Thermal efficiency, expander Power, Pump input power, evaporator capacity and condenser capacity matrix as follows:

$$ORC\_Results = \begin{pmatrix} \text{"Mass Flow Rate, m1, [kg/s]"} & 0.308 \\ \text{"Thermal Efficiency,η, [\%]"} & 6.242 \\ \text{"Turbine Power, Wt, [kW]"} & 5.3 \\ \text{"Pump Power, Wp, [kW]"} & 0.3 \\ \text{"Evaporator Capacity, QE, [kW]"} & 80.104 \\ \text{"Condenser Capacity, QK, [kW]"} & 75.104 \end{pmatrix}$$

Matrix of properties of different points as follow:

$$Points\_Properties = \begin{pmatrix} \text{"No"} & \text{"Temperature [C]"} & \text{"Enthalpy, [kJ/kg]"} & \text{"State"} \\ \text{"1"} & 39.944 & 252.494 & \text{"saturated liquid"} \\ \text{"2"} & 40.585 & 253.469 & \text{"subcooled liquid"} \\ \text{"3"} & 124 & 513.453 & \text{"superheated vapor"} \\ \text{"4"} & 102 & 496.251 & \text{"superheated vapor"} \end{pmatrix}$$

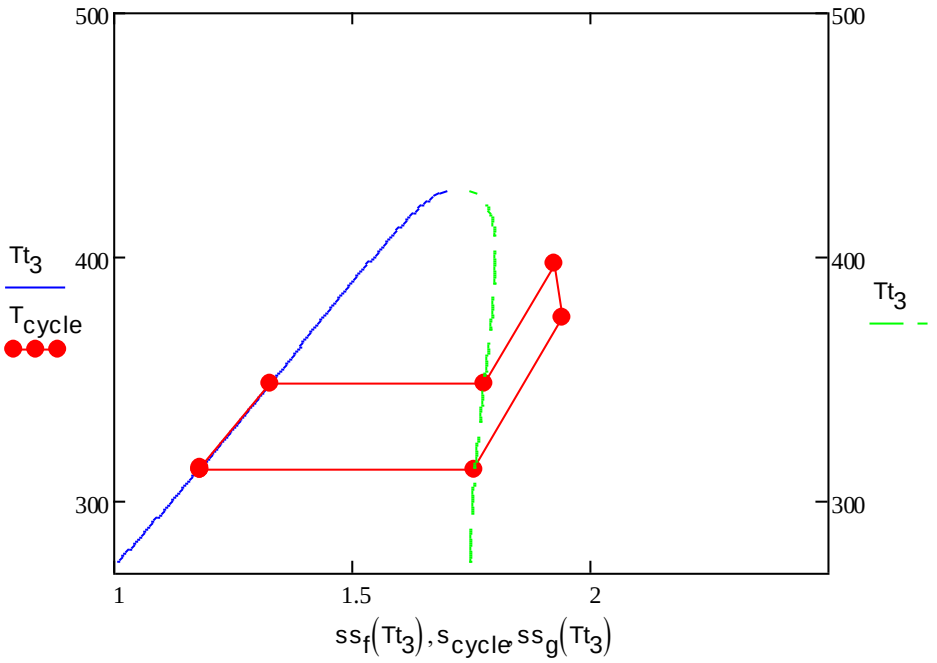


**Figure 4.5:** T-s diagram of Analyzed ORC

*Carnot efficiency*

Carnot efficiency of the system is 25% calculated by the followıng formula:

$$Carnot\ Efficiency(\%): (1 - \frac{T_L}{T_H}) \times 100 \tag{4.1}$$

## 4.2 Heat Exchangers Results

In this subchapter, the performance of condenser when fluid passes expansion valve in the expansion process, pressure drop results for two different chevron angles and their effects on cycle efficiency, effect of cold source temperature on condenser and evaporation temperature effect on the total area of evaporator and condenser is examined.

### 4.2.1 Chevron angle 45° and 60° heat transfer performance comparison

Plates with both chevron angle 45° and 60° are widely used in HEXs. In this section, a comparison is made between their performances in our design condition. In below matrixes results of the HTC for every region of the process using related correlations for both angles are presented.

HTC values for plate with 45° chevron angle

$$HTC = \begin{pmatrix} \text{"HEX"} & \text{"Refrigerant side HTC"} & \text{"Water side HTC"} \\ \text{"Superheater region"} & 641.785 & 7.351\times 10^3 \\ \text{"Evaporator region"} & 2.343\times 10^4 & 7.253\times 10^3 \\ \text{"Preheater region"} & 565.767 & 6.711\times 10^3 \\ \text{"Desuperheater region"} & 889.993 & 1.02\times 10^4 \\ \text{"Condenser1 region"} & 1.966\times 10^3 & 9.109\times 10^3 \\ \text{"Condenser 2"} & 1.989\times 10^3 & 7.139\times 10^3 \end{pmatrix}$$

HTC values for plate with 60° chevron angle

$$HTC = \begin{pmatrix} \text{"HEX"} & \text{"Refrigerant side HTC"} & \text{"Water side HTC"} \\ \text{"Superheater region"} & 803.476 & 9.424\times 10^{3} \\ \text{"Evaporator region"} & 3.147\times 10^{5} & 9.299\times 10^{3} \\ \text{"Preheater region"} & 722.39 & 8.591\times 10^{3} \\ \text{"Desuperheater region"} & 1.201\times 10^{3} & 1.447\times 10^{4} \\ \text{"Condenser1 region"} & 2.629\times 10^{3} & 1.287\times 10^{4} \\ \text{"Condenser 2"} & 2.712\times 10^{3} & 6.876\times 10^{3} \end{pmatrix}$$

From above matrixes we can deduce that generally plates with 60° chevron angle have higher HTC and better heat transfer performance in all of the processes.

### 4.2.2 Condenser performance in different expansion processes

In start-up condition or any other condition, that fluid is required to pass the expansion valve in expansion process, condenser and desuperheater performances are investigated in this section.

*Performance of desuperheater and condenser when flow passes expander*

In design condition, fluid passes expander in the expansion process. $T_4$ is the inlet temperature of desuperheater. Theoretical transferred heat in this mode can be calculated by the equation 3.9. Results in Table 4.1 and Table 4.2 are obtained by using the single-phase correlation equations 2.9 to 2.14.

**Table 4.1:** HEX 1 ,heat transfer parameters when fluid passes expander

| HEX 1 (Desuperheater and condenser) | Desuperheater | Condenser1 |
|---|---|---|
| Water Mass flow rate (Kg/s) | 1.797 | 1.797 |
| Length(m) | 0.146 | 0.32 |
| Overall heat transfer coefficient U (W/m2.k) | 863.69 | 1400 |
| Transferred heat rate (kW) | 19.281/19.281 (actual/theoretical) | 27.682 |
| HEX efficiency | 0.62 | 0.247 |

**Table 4.2:** HEX 2, heat transfer parameters when fluid passes expander

| HEX 2 (Condenser) | Condenser 2 |
|---|---|
| Water Mass flow rate (kg/s) | 0.753 |
| Length(m) | 0.466 |
| Overall heat transfer coefficient U (W/m2.k) | 1298 |
| Transferred heat rate (kW) | 28.149 |
| HEX efficiency | 0.598 |

*Performance of desuperheater and condenser when flow passes expansion valve*

When fluid passes expansion valve in the expansion process 118.5°C is the inlet temperature of desuperheater. Theoretical transferred heat in this mode can be calculated by the equation 3.10. Results related to actual transferred heat in HEX are obtained by using the single-phase correlation equations 2.9 and 2.14 and displayed in Table 4.3 and Table 4.4.

**Table 4.3:** HEX 1, heat transfer parameters when fluid passes expansion valve

| HEX 1 (Desuperheater and condenser) | Desuperheater | Condenser1 |
|---|---|---|
| Water Mass flow rate (kg/s) | 1.797 | 1.797 |
| Length(m) | 0.159 | 0.309 |
| Overall heat transfer coefficient U (W/m2.k) | 899.63 | 1401 |
| Transferred heat rate actual/theoretical (kW) | 24.602/24.582 | 26.711 |
| HEX efficiency | 0.882 | 0.238 |

**Table 4.4:** HEX 2, heat transfer parameters when fluid passes expansion valve

| HEX 2 (Condenser) | Condenser 2 |
|---|---|
| Water Mass flow rate (kg/s) | 0.82 |
| Length(m) | 0.466 |
| Overall heat transfer coefficient (U) | 1311 |
| Transferred heat rate (kW) | 29.231 |
| HEX efficiency | 0.571 |

From above results, we can conclude that to have fully condensed fluid at the exit of condenser 2 cold water mass flow rate should be increase from 0.752 kg/s to 0.82 kg/s.

### 4.2.3 Pressure loss effect on HEXs on cycle efficiency

In this section pressure drop is calculated for both chevron angles of 45° and 60° by using related correlations and needed pump power is calculated by using equation 2.32 and efficiency by equation 3.9. Extra needed pump power and its effect on efficiency are indicated in table 11.

Pressure drop results for 45 degrees chevron angle

$$HEX\_RESULTS\_P = \begin{pmatrix} \text{"HEX"} & \text{"Refrigerant side (Pa)"} & \text{"Water side (Pa)"} \\ \text{"Superheater region"} & 1.267\times 10^{3} & 500.226 \\ \text{"Evaporator region"} & 1.131\times 10^{4} & 115.842 \\ \text{"Preheater region"} & 16.687 & 154.765 \\ \text{"Desuperheater region"} & 4.208\times 10^{3} & 2.468\times 10^{3} \\ \text{"Condenser1 region"} & 1.357\times 10^{3} & 4.502\times 10^{3} \\ \text{"Condenser"} & 2.101\times 10^{3} & 6.969\times 10^{3} \\ \text{"Total loss"} & 2.026\times 10^{4} & 1.471\times 10^{4} \end{pmatrix}$$

Pressure drop results for 60 degrees chevron angle:

$$HEX\_RESULTS\_P = \begin{pmatrix} \text{"HEX"} & \text{"Refrigerant side (Pa)"} & \text{"Water side (Pa)"} \\ \text{"Superheater region"} & 2.904\times 10^{3} & 1.226\times 10^{3} \\ \text{"Evaporator region"} & 1.906\times 10^{4} & 234.152 \\ \text{"Preheater region"} & 28.799 & 270.673 \\ \text{"Desuperheater region"} & 9.493\times 10^{3} & 6.019\times 10^{3} \\ \text{"Condenser1 region"} & 1.747\times 10^{3} & 1.319\times 10^{4} \\ \text{"Condenser"} & 2.544\times 10^{3} & 3.372\times 10^{3} \\ \text{"Total loss"} & 3.577\times 10^{4} & 2.431\times 10^{4} \end{pmatrix}$$

Refrigerant side frictional pressure loss for two chevron angles and their effects are listed in the following Table 4.5:

**Table 4.5:** Total pressure loss HEXs and needed extra pump power

| Chevron angle | Total Pressure loss [kPa] | Added pump power [kW] | Resulted cycle efficiency [%] | Cycle efficiency drop percentage [%] |
|---|---|---|---|---|
| 45° | 20.01 | 0.0142 | 6.229 | 0.444 |
| 60° | 35.77 | 0.0287 | 6.207 | 0.560 |

### 4.2.4 Effects of cold source temperature change

Since cold water temperature can vary through different months of the year. In this part, effect of the cold source temperature change on water mass flow rate for

condenser is investigated. The mass flow rate of water is calculated in a way to avoid subcooling for temperatures lower than designed or incomplete condensation in condenser for temperatures higher than designed.

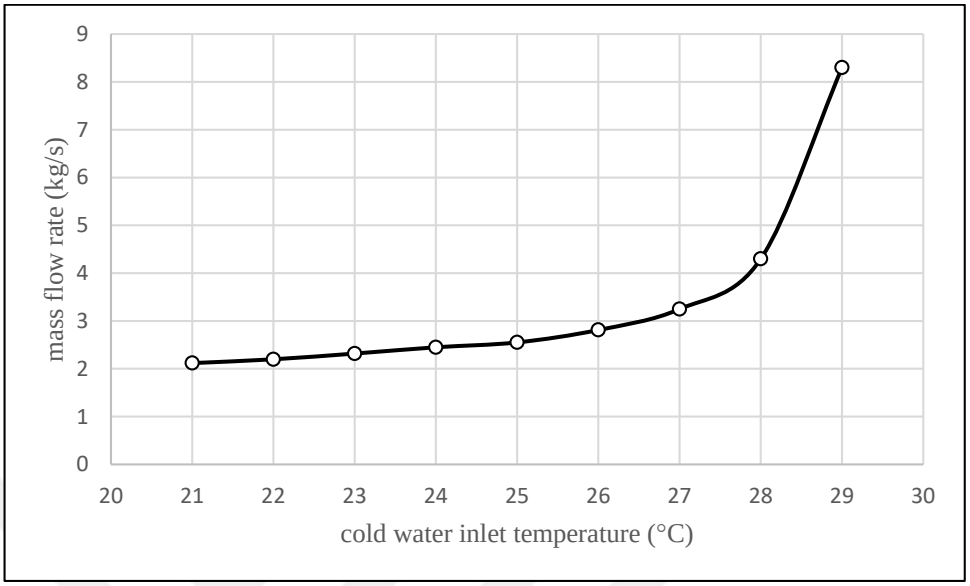


**Figure 4.6:** Cold water temperature effect on mass flow rate

### 4.3 Change of Required Area in Different Evaporation Temperatures

In order to analyze the effect of increased evaporation temperature on the size of evaporator and condenser (pure evaporation and pure condensation), HEXs with minimum 0.5 efficiencies are considered for analyzing. By neglecting errors for use of correlations in different evaporation temperature, required areas for output power are calculated.

Diagrams below represents the required area and efficiency change for evaporator and condenser as the evaporation temperature increases.

Fixed parameters in this analysis are output power, hot and cold source temperature, mechanical efficiencies of pump and expander and condensation temperature.

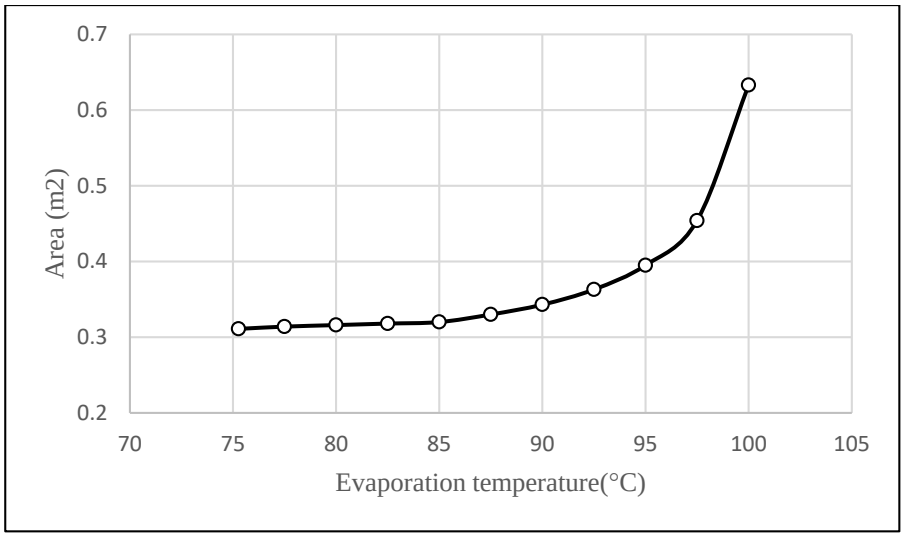


**Figure 4.7:** Effect of evaporation temperature change on evaporator area for output power (Fixed parameters: $\boldsymbol{T_H, T_C, \eta_{pump}, \eta_{expander}, T_{Cond}, W_{Exp}}$)

For the same power output by increasing evaporation temperature, NTU value increases by raising evaporation temperature, thus HEX efficiency value for evaporator also increases (NTU is the only effecting parameter in efficiency equation).

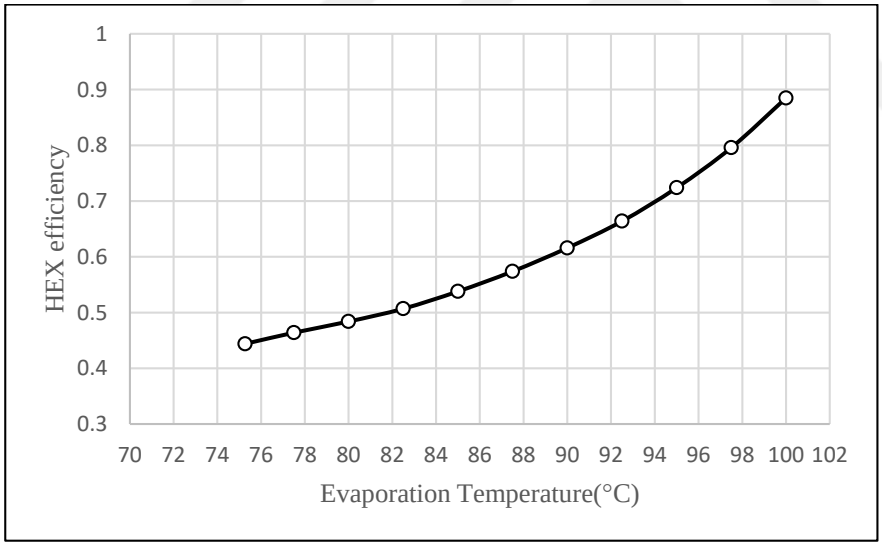


**Figure 4.8:** Effect of evaporation Temperature on evaporator efficiency

In case of the condenser (pure condensation), by increasing evaporation temperature overall cycle efficiency increases, needed condenser capacity decreases. So need of the area for condenser also decreases.

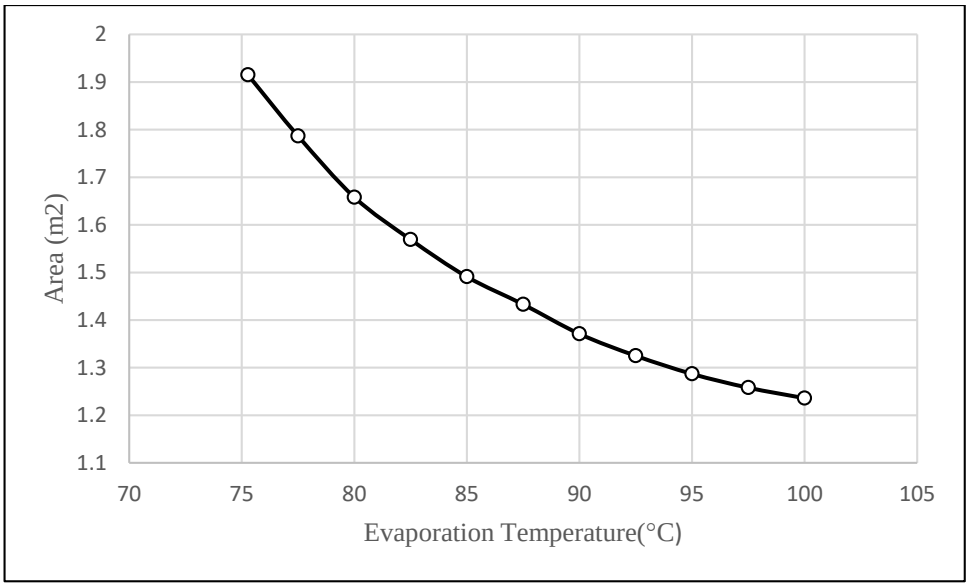


**Figure 4.9:** Effect of evaporation temperature on condenser area (Fixed parameters: $T_H, T_C, \eta_{pump}, \eta_{expander}, T_{Cond}, W_{Exp}$)

Similar to evaporator with increasing of evaporation temperature NTU value which is the sole affecting parameter in HEX efficiency equation increases and consequently by increasing evaporation temperature, the efficiency of condenser increases.

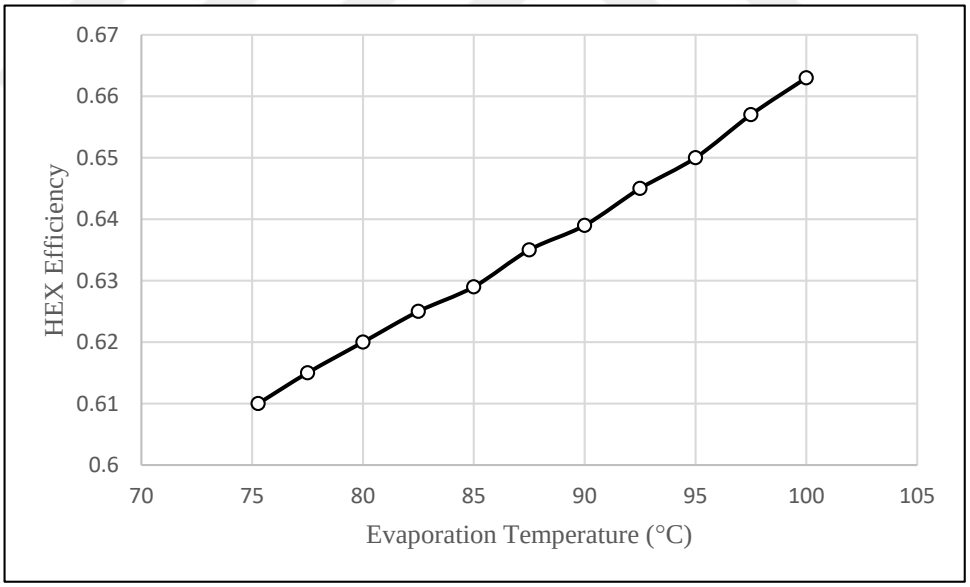


**Figure 4.10:** Evaporation temperature effect on condenser efficiency

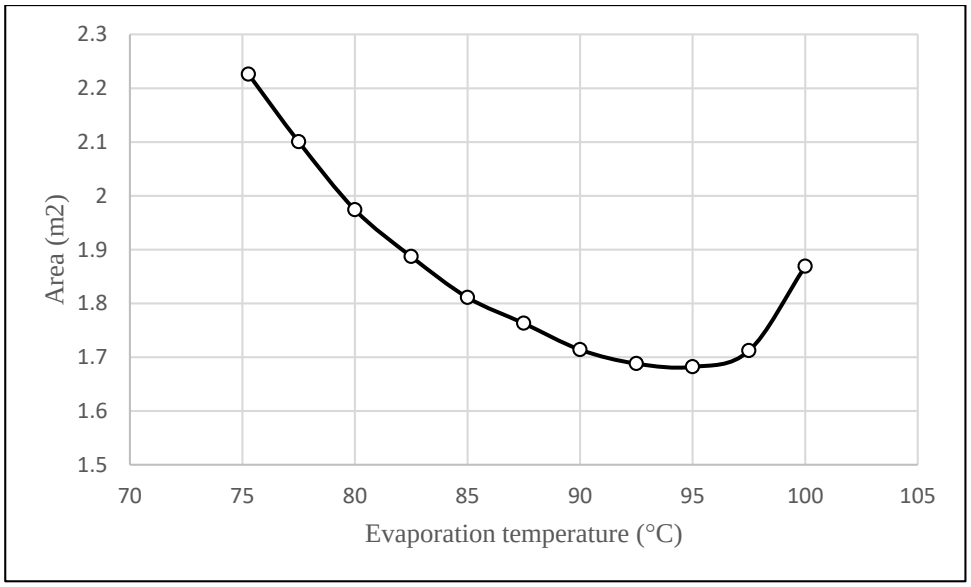


**Figure 4.11:** Total area for condenser and evaporator for power output (Fixed parameters: $T_H, T_C, \eta_{pump}, \eta_{expander}, T_{Cond}, W_{Exp}$)

From the figure above, we can deduce that raising evaporation temperature up to 95 °C in our case can optimize overall HEX area and as a result, optimize the capital cost of ORC unit.

## 5. CONCLUSION

An ORC system of 5 kW net power output with PHE as evaporator and condenser is modeled. A code in Mathcad program is developed to perform thermal analysis. In first part of the results, required capacity for each component, the required fluid mass flow rate of R245fa, cycle thermal efficiency, etc. are obtained. Effect of isentropic efficiencies of pump and expander are examined, besides, evaporation and condensation temperatures effect on cycle thermal efficiency are also investigated. In the second part of results, with the help of correlations performances of two chevron angles are compared with each other, HEX performance in design and some off-design conditions are examined and finally the effect of increasing of evaporation temperature on the total area of HEXs is investigated.

Five kW ORC system operation parameters are listed in the following Table 5.1:

**Table 5.1:** ORC system characteristics overview

| Parameter | Value |
|---|---|
| Hot source temperature [°C] | 125 |
| Hot water mass flow rate [kg/s] | 0.901 |
| Cold source temperature [°C] | 25 |
| Cold water mass flow rate (kg/s) | 2.54 |
| Cycle thermal efficiency [%] | 6.242 |
| Refrigerant mass flow rate [kg/s] | 0.308 |
| Evaporator capacity [kW] | 80.104 |
| Condenser capacity [kW] | 75.104 |
| Expander mechanical efficiency [%] | 75 |
| Pump mechanical efficiency [%] | 35.6 |

Developed Mathcad code features are listed as follow:

- Any other refrigerants can be selected for analysis.
- PHEs with different dimensions can be selected for analysis.
- Different design parameters can be chosen for analysis such as cold and hot source temperatures
- Any other correlations can be used simply by replacing the correlations in the built-in functions for HTCs.

Conclusions made in this study listed down below:

- Better cycle thermal efficiency can be obtained by increasing of the expander and pump isentropic efficiency, evaporation temperature and by decreasing of condensation temperature.
- Higher HTCs are possible with 60° chevron angle plates; however, they have also higher pressure drop comparing the plates with 45° chevron angle.
- Pressure loss in HEX can decrease cycle efficiency by 0.444% for HEX with 45° angle plates and 0.560% for HEX with 60° angle plates.
- Cold water temperature range for inlet of the desuperheater and condenser varies from 21 to 28°C. If the water temperature passes over 28°C, required water mass flow rate to have fully condensed fluid at condenser outlet exponentially increases, thus extra condenser should be used for temperatures over 28°C in order to have fully condensed R245fa at the outlet of the condenser for temperatures over 28°C.
- When working fluid completely passes expansion valve (For example: during start-up), mass flow rate of cold water shall increase from 2.547 kg/s to 2.617 kg/s to have fully condensed R245fa at the condenser outlet.
- Required evaporator area gradually as the evaporation temperature increases. However because of better efficiency of the cycle, by increasing the evaporation temperature, required condenser area decreases. We can conclude that optimum total area in our case is possible at 95°C.

- Increasing evaporation temperature from about 75°C to 95°C can reduce the total area of evaporator and condenser by 24.44%.

Suggestions:

- In our work, only the control cold water mass flow rate is investigated. Therefore, study of the control of the system is incomplete and further study with utilization of an automation system is required.
- Start-up and shutdown of the system are two scenarios that are required to be analyzed. To examine these scenarios, present work can be extended by formulating time-dependent mathematical formulation for some of the units. For this matter, different equipment of control such as measuring sensors and various automation equipment can be assigned.

  We conclude that optimum overall area for evaporator and condenser can be obtained at 95°C. However, the used correlations are the limiting factor for obtaining more accurate results since they may not ensure precise results at this operating condition. So more exact results can be obtained by employing more accurate correlations.

## 6. REFERENCES


[1] **STEEN, M.** Greenhouse gases emissions from fossil fuel fired powered stations, joint research center, European commission

[2] **Zhai, H., An, Q., Lin, S., Lemort V., Quoilin, S.** (2017) Categorization and analysis of heat sources for organic Rankine cycle systems

[3] **Macci**, **E.**Theoretical basis of Organic Ranike cycle, organic rankine power cystems chapter 1

[4] **Url-1** <https://www.brighthubengineering.com/power-plants/72369-compare-the-efficiency-of-different-power-plants/>, date received: 20.03.2018

[5] **Bronicky, L.V.** History of Organic rankine cycle systems (chapter 2), Organic Rankine cycle power systems

[6] **Kheiri, A., Feidt, M., Pelloux-Prayer, S.** Thermodynamic and economic optimizations of a waste heat to power plant driven by a subcritical ORC (Organic Rankine Cycle) using pure or zeotropic working fluid. Energy 2014;78:622–38.

[7] **Imran, M., Usman M., Park. B.S., Yang, Y.** Comparative assessment of Organic Rankine Cycle integration for low temperature geothermal heat source applications, Energy 102 ,473–490.

[8] **Imran, M., Park, B.S., Kim, H.J., Lee, D.H., Usman, M., Heo**, **M.** Thermo economic optimization of Regenerative Organic Rankine Cycle for waste heat recovery applications, Energy Convers. Manage. 87 107–118.

[9] **Imran, M., Usman M., Park, B.S., Kim, H.J., Lee D.H.**. Multi-objective optimization of evaporator of organic Rankine cycle (ORC) for low temperature geothermal heat source, Appl. Therm. Eng. 80(5) 1–9.

[10] **Jumel, S., Feidt, M., Le, V.L., Kheiri,. A.** Working fluid selection and performance comparison of subcritical and supercritical organic Rankine cycle (ORC) for low temperature waste heat recovery

[11] **Imran, M., Usman M., Yang, Y., Park, B.S. (2017).**Flow boiling of R245fa in the brazed plate heat exchanger: Thermal and hydraulic performance assessment

[12] **Luo, X., Liang, Z., Guo, G., Wang, C., Chen Y., Ponce-Ortega, J.M., El-Halwagi, M.M. (2017).** Thermo-economic analysis and optimization of a zoetropic fluid organic Rankine cycle with liquid-vapor separation during condensation

[13] **Leibowitz, H., Smith, I., Stosic, N.** Cost effective small scale orc systems for power recovery from low grade heat sources, ASME International Mechanical Engineering Congress and Exposition 2006; Pages 5-6.

[14] **Rowshanzadeh, R.,** Performance and cost evaluation of Organic Rankine Cycle at different technologies

[15] **Schuster, A., Karellas, S., Kakaras, E., Spliethoff, H. (2009)** Energectic and economic investigation of Organic Rankine Cycle application.

[16] **Url-2** <http://www.enerjiatlasi.com/elektrik-fiyatlari/> date retrieved:20.04.2018

[17] **Url-3** <http://www.infinityturbine.com/> date retrieved: 15.02.2018

[18] **Yari, M., Mehr, A.S., Zare, V., Mahmoudi, S.M.S., Rosen, M.A. (2015)** Exergoeconomic comparison TLC, ORC and Kalina cycle using low-grade heat source

[19] **Vidhi, R., Kuravi, S., Goswami, Y., Stefanakos, E., and Sabau, A.** Organic Fluids in a Supercritical Rankine Cycle for Low Temperature Power Generation (2013)

[20] **Bell, I.H., Lemmon, E.W.** Organic fluids for Organic Rankine Cycle systems: classification and calculation of thermodynamic and transport properties- 4.9.2

[21] **Korkmaz, E.D., Serpen, U., Satman, A.** (2012). TURKEY'S GEOTHERMAL ENERGY POTENTIAL: UPDATED RESULTS

[22] **Url-4** <https://www.mgm.gov.tr/veridegerlendirme/sicaklik-analizi.aspx?s=m> date retrieved: 10.03.2018

[23] **Quoilin, S., Broek, M.V.Den., Declaye, S., Dewallef, P., Lemort, V.** Techno-economic survey of Organic Rankine Cycle(ORC) systems

[24] **Url-5** <https://www.boconline.co.uk/internet.lg.lg.gbr/en/images/sg_238-r245-%20fa-pentafluoropropane-v1.3410_39652.pdf?v=3.0> date retrieved:05.03.2018

[25] **Ramesh, K.S., Sekulic, D.** Fundamentals of Heat exchangers design-Page 515-516.

[26] **Url-6** <https://www.alfalaval.no/microsites/platevarmevekslere-med-pakning/typer/> date retrieved:10.02.2018

[27] **Lemort, V., Legros, A.** Positive displacement expanders (chapter 12), Organic Rankine cycle power systems

[28] **Gnutek, Z., Kolasin´ski, P.**. The Application of Rotary Vane Expanders in Organic Rankine Cycle Systems—Thermodynamic Description and Experimental Results.

[29] **Url-7** <https://en.wikipedia.org/wiki/Mathcad> date retrieved: 20.03.2018

[30]**Url-8** <https://www.energy.gov/sites/prod/files/2016/07/f33/R27%20-%20Waste%20Heat-to-Power%20Using%20Scroll%20Expander%20for%20Organic%20Rankine%20Bottoming%20Cycle%20TIAX%202016_compliant.pdf> date retrieved: 10.03.2018

[31]**Url-9** <https://www.alfalaval.com/globalassets/documents/industries/refrigeration/brazed-plate-heat-exchangers.pdf> date retieved: 15.02.2018

[32] **Tian, H., Chang, L., Gao, Y., Shu, G., Zhao, M., Yan, N.** Thermo-economic analysis of zeotropic mixtures based on siloxanes for engine waste heat recovery using a dual-loop organic Rankine cycle (DORC)

[33] **Carraro, G., Pallis, P., D.Leontaritis, A., Karellas, S., Vourliotis, P., Rech, S., lazaretto, A.** Experimental performance evaluation of a multi-diaphragm pump of a micro-ORC system (2017)

[34] **Ma, Z., Bao H., Roskilly, A.P.** Dynamic modelling and experimental validation of scroll expander for small scale power generation system (2017)

**CURRICULUM VITAE**

**Name Surname** **:** Yashar AMROLLAHI FARZI

**Place and Date of Birth** **:** Tabriz-Iran, 27/08/1991

**E-Mail** **:** y.amrollahi@live.com

**EDUCATION** **:**

- **B.Sc.** **:** 2014, Shahid Madani Azarbaijan University, Mechanical Engineering (Heat Fluid Approach)